NASA-TM-85959 19840025035

Second- and Third-Order Upwind Difference Schemes for Hyperbolic Conservation Laws

Jaw-Yen Yang

July 1984

NASA
National Aeronautics and
Space Administration

NF00818

N84-33106 #

Second- and Third-Order Upwind Difference Schemes for Hyperbolic Conservation Laws

Jaw-Yen Yang, Ames Research Center, Moffett Field, California

NASA

National Aeronautics and
Space Administration

Ames Research Center
Moffett Field, California 94035

N84-33106 #

SUMMARY

Second- and third-order two time-level five-point explicit upwind-difference schemes are described for the numerical solution of hyperbolic systems of conservation laws and are applied to the Euler equations of inviscid gas dynamics. Nonlinear smoothing techniques are used to make the schemes total variation diminishing. In this method both hyperbolicity and conservation properties of the hyperbolic conservation laws are combined in a natural way by introducing a normalized Jacobian matrix of the hyperbolic system. Entropy satisfying shock transition operators (which are consistent with the upwind differencing) are locally introduced when transonic shock transition is detected. Schemes thus constructed are suitable for shock-capturing calculations. The stability and the global order of accuracy of the proposed schemes are examined. Numerical experiments for the inviscid Burgers' equation and the compressible Euler equations in one- and two-space dimensions involving various situations of aerodynamic interest are included and compared. Numerical results using second-order schemes indicate that the stationary shock can be captured within (at most) two transition zones and the contact surface can be accurately resolved, and are comparable with those obtained by van Leer's and Harten's high resolution schemes. Preliminary results for one-dimensional problems using the third-order scheme are presented.

1. INTRODUCTION

The hyperbolic conservation equations of inviscid gas dynamics have two mathematical properties which are of great significance in the design of a numerical method. First, for nonlinear hyperbolic partial differential equations, the theory of characteristics provides the correct directional signal propagation information and physical domain of dependence and has long been recognized as a natural procedure for solving the equations (refs. 1 and 2). Second, the conservation-law form of the equations permits one to construct conservative shock-capturing numerical schemes (refs. 3-5) due to a theorem of Lax and Wendroff (ref. 3).

A first-order accurate upwind finite difference scheme was developed for solving the nonlinear hyperbolic equations by Courant, Isaacson and Rees in 1952 (ref. 1). Their method was based on the normal or characteristic form of the quasi-linear first-order hyperbolic system. With the idea in mind of preserving the domain of dependence, the spatial derivative in each direction of the characteristic form was approximated by either a first-order forward or backward finite difference quotient depending upon whether the local eigenvalue (characteristic speed) is negative or positive. The notion of eigenvalue splitting was introduced to provide the automatic switching for constructing uniform upwind finite difference schemes.

Attempts to construct finite difference schemes by using both the conservation property and hyperbolicity property of the hyperbolic conservation equations were presented by Godunov (ref. 6) and by Steger and Warming (ref. 7). Recently, several upwind flux difference splitting methods have been proposed (refs. 8-12) for solving

hyperbolic conservation equations. A review of some recent developments in one-sided (upwind) difference schemes has been reported by Harten, Lax, and van Leer (ref. 13).

In references 14 and 15, a first-order upwind flux difference splitting method was developed for hyperbolic systems of conservation laws and was applied to the Euler equations of inviscid gas dynamics. First-order explicit and implicit schemes are described and can be viewed as the corresponding development for hyperbolic conservation laws as the Courant-Isaacson-Rees (ref. 1) method for the hyperbolic equations in quasi-linear form. The scheme has similar desirable shock calculation properties of Osher's scheme (ref. 10) but the integration path used in his method is avoided. In comparison, the special averaging technique used in Roe's scheme (ref. 8) was replaced by a simpler formulation.

It is well known that first-order accurate schemes are too diffusive, but classical higher-order schemes, while giving better resolution of the discontinuities of the solution, exhibit spurious oscillations around such points (e.g., the Lax-Wendroff scheme (ref. 3), the Fromm scheme (ref. 16), and the Warming-Beam scheme (ref. 17). In recent years, effort has been put into obtaining second- or higher-order schemes which give high resolution while remaining total variation diminishing or nonincreasing (TVD), a notion introduced by Harten (ref. 18).

The present study is a sequel to the work contained in references 14 and 15. Second- and third-order (in space and time) accurate explicit two time-level five-point upwind difference schemes are described for the numerical solution of hyperbolic systems of conservation laws and are applied to the compressible Euler equations of inviscid gas dynamics. Nonlinear smoothing techniques (or flux limiters) are used to make the schemes "monotonicity-preserving" (or TVD). Many such nonlinear smoothing techniques are available. Recently, a systematic study on flux limiters including those proposed by van Leer (ref. 19), Roe (ref. 20), Harten (ref. 18), and Chakravarthy and Osher (ref. 21) has been reported by Sweby (ref. 22). Implicit TVD schemes have been presented by Harten (ref. 23) and Yee, Warming, and Harten (ref. 24).

Section 2 begins with a brief review of the basic notion and the first-order characteristic flux difference splitting method described in references 14 and 15. In Section 3, shock transition operators which allow entropy-satisfying shock transitions are described in accord with the principle of upwind differencing. In Section 4, five-point second-order upwind difference schemes for single conservation laws and for systems are given. They are constructed based on Fromm's zero-average phase-error scheme (ref. 16). A nonlinear smoothing technique devised by van Leer (ref. 19) is used to make the scheme monotonicity-preserving. We also describe a second-order scheme obtained by applying our first order accurate scheme to a modified flux function similar to the one devised by Harten (ref. 18). In Section 5, we extend the second-order upwind scheme using van Leer's (ref. 19) flux limiter to a third-order upwind scheme based on the characteristic flux difference splitting concept. Stability and accuracy of the second- and third-order schemes are examined in Section 6. Applications to the Euler equations of gas dynamics are illustrated in Section 7. In Section 8, numerical experiments for the inviscid Bergers' equation and the Euler equations in one- and two-space dimensions involving various situations of aerodynamic interest are considered and the results are discussed. Concluding remarks are made in Section 9.

2

2. CHARACTERISTIC FLUX DIFFERENCE SPLITTING

To illustrate the basic notions, we consider numerical solutions of a hyperbolic system of conservation laws in one space dimension

$$\partial_t U + \partial_x F = 0 \qquad\qquad (2\text{-}1a)$$

subject to the initial data

$$U(x,0) = \phi(x) , \qquad -\infty < x < \infty \qquad\qquad (2\text{-}1b)$$

where $\phi(x)$ is a given function and $U = (u_1, u_2, \ldots, u_m)^T$ and $F = (f_1, f_2, \ldots, f_m)^T$ are m-component column vectors. Equation (2-1a) can be rewritten as a quasi-linear system

$$\partial_t U + A \partial_x U = 0 \qquad\qquad (2\text{-}2)$$

where A is the Jacobian matrix $\partial F / \partial U$. We require that the sytem of equations (2-1a,b) be hyperbolic in the sense that the Jacobian matrix A has real eigenvalues and a complete set of eigenvectors. Let the eigenvalues of A be denoted by $a_1, a_2, \ldots, a_m$ with corresponding right eigenvectors $r_1, r_2, \ldots, r_m$. Defining $Q^{-1}(U)$ to be the matrix whose jth column is $r_j(U)$, it then follows that

$$Q \Lambda Q^{-1} = A \qquad\qquad (2\text{-}3)$$

where Λ is a diagonal matrix with the eigenvalues a_ℓ as its elements and the norms of Q and Q^{-1} are uniformly bounded. By using equation (2-3), equation (2-2) can be put in the following characteristic form:

$$Q^{-1} \partial_t U + \Lambda Q^{-1} \partial_x U = 0 \qquad\qquad (2\text{-}4)$$

For the purpose of analysis, we assume that the coefficient matrix A is "frozen," that is, constant. By virtue of equations (2-3) and (2-4) one can transform equation (2-4) to the uncoupled system:

$$\partial_t v_\ell + a_\ell \partial_x v_\ell = 0 , \qquad \ell = 1, 2, \ldots, m \qquad\qquad (2\text{-}5)$$

by defining a new characteristic vector $V = (v_1, v_2, \ldots, v_m)^T = Q^{-1} U$. The eigenvalues are real and equation (2-5) is equivalent to a set of uncoupled scalar wave equations. For simplicity, the subscript ℓ will be dropped for the remainder of this section.

Define a uniform computational mesh $\{x_j, t^n\}$, with mesh sizes Δx and Δt. The discrete representation of $v(x,t)$ on the mesh is v_j^n and $\lambda = \Delta x / \Delta t$ is the mesh ratio.

A first-order upwind difference scheme for solving equation (2-5) was introduced by Courant, Isaacson, and Rees (ref. 1)

$$v_j^{n+1} = v_j^n - \lambda a \begin{cases} \Delta_{j-(1/2)} v^n , & a \geq 0 \\ \Delta_{j+(1/2)} v^n , & a < 0 \end{cases} \tag{2-6}$$

We can combine the above scheme into one uniform scheme by splitting the eigenvalue a into the positive part a^+ and negative part a^-.

$$v_j^{n+1} = v_j^n - \lambda a^+ \Delta_{j-(1/2)} v^n - \lambda a^- \Delta_{j+(1/2)} v^n \tag{2-7}$$

where

$$a = a^+ + a^- \tag{2-8}$$

and

$$a^+ = (a + |a|)/2 = \max(a,0) , \quad a^- = (a - |a|)/2 = \min(a,0) \tag{2-9}$$

with

$$\Delta_{j-(1/2)} v^n = v_j^n - v_{j-1}^n$$

Extending the above procedure to system equation (2-2), one obtains

$$U_j^{n+1} = U_j^n - \lambda A_{j-(1/2)}^+ \Delta_{j-(1/2)} U^n - \lambda A_{j+(1/2)}^- \Delta_{j+(1/2)} U^n \tag{2-10}$$

with

$$A = A^+ + A^- \tag{2-11}$$

where

$$A^\pm = Q \Lambda^\pm Q^{-1} \tag{2-12}$$

and

$$\Lambda = \Lambda^+ + \Lambda^- \tag{2-13}$$

where

$$\Lambda^\pm = \text{diag}\{a_\ell^\pm\} \tag{2-14}$$

In references 14 and 15, we presented a corresponding development for hyperbolic systems of conservation laws equation (2-1) by using the following approach: For the purpose of upwind differencing, we will rewrite equation (2-1a) as

$$\partial_t U + (\hat{A}^+ + \hat{A}^-) \partial_x F = 0 \tag{2-15}$$

4

where $\hat{A}^{\pm}(U) = Q\hat{\Lambda}^{\pm}Q^{-1}$ remain to be defined but are required to satisfy

$$\hat{A}^+ + \hat{A}^- = I \qquad (2\text{-}16)$$

$\hat{A}^+$ and $\hat{A}^-$ are closely related to matrices A^+ and A^- of equation (2-11) and carry the hyperbolicity property of the equations through the expression

$$\hat{A}^+ = Q\text{diag}\{\hat{a}_\ell^+\}Q^{-1} \quad \text{and} \quad \hat{A}^- = Q\text{diag}\{\hat{a}_\ell^-\}Q^{-1} \qquad (2\text{-}17)$$

The "normalized" eigenvalues $\hat{a}_\ell^{\pm}$ are defined as

$$a_\ell^{\pm} = \frac{a_\ell^{\pm}}{a_\ell} = \frac{1}{2} \pm \frac{1}{2}\,\text{sgn}(a_\ell)\,, \quad \text{if} \quad a_\ell \neq 0 \qquad (2\text{-}18)$$

For $a_\ell = 0$, which corresponds to a sonic point, special treatment is needed. Suppose that the eigenvalue a_ℓ is equal to zero at the nodal point J. Then in order to be consistent with upwind differencing we take

$$\hat{a}_J^{\pm} = \hat{a}_{J\pm1}^{\pm} \quad \text{if} \quad a_J = 0 \qquad (2\text{-}19)$$

This will exclude stationary expansion shocks and make the scheme entropy satisfying. Further discussion on this aspect will be given in the next section.

An explicit first-order upwind difference scheme for equation (2-15) can be expressed as

$$U_j^{n+1} - U_j^n = -\lambda\hat{A}_{j-(1/2)}^+\Delta_{j-(1/2)}F^n - \lambda\hat{A}_{j+(1/2)}^-\Delta_{j+(1/2)}F^n \qquad (2\text{-}20)$$

For steady-state calculations, a corresponding implicit scheme is given by

$$[I + \lambda\hat{A}_{j-(1/2)}^+\Delta_{j-(1/2)}A^n + \lambda\hat{A}_{j+(1/2)}^-\Delta_{j+(1/2)}A^n]\Delta U^n = \text{RHS} \qquad (2\text{-}21)$$

of (2-20), where $\Delta U^n = U^{n+1} - U^n$.

The nodal point at which the coefficient matrices are evaluated is relevant to the numerical schemes thus generated. We list two ways of defining the values of $A_{j\pm(1/2)}^{\pm}$ used in the present study:

$$(i)\hat{A}_{j-(1/2)}^+ = (\hat{A}_{j-1}^+ + \hat{A}_j^+)/2\,, \quad \hat{A}_{j+(1/2)}^- = (\hat{A}_j^- + \hat{A}_{j+1}^-)/2 \qquad (2\text{-}22)$$

$$(ii)\hat{A}_{j-(1/2)}^+ = \hat{A}^+[(U_{j-1} + U_j)/2]\,, \quad \hat{A}_{j+(1/2)}^- = \hat{A}^-[(U_j + U_{j+1})/2] \qquad (2\text{-}23)$$

We wish to point out that the averages given by (2-22) or (2-23) are only correct for mesh intervals in which the eigenvalues are of the same sign. For mesh intervals which cover regions of transonic shock transitions (i.e., regions where eigenvalues switch signs), the above formulas are not consistent with the idea of preserving the domain of dependence.

Examples for constructing matrices $\hat{A}^{\pm}$ for the Euler equations of gas dynamics will be given later.

It is noted that the following relations hold for the normalized Jacobian matrix $\hat{A}^{\pm}$:

$$\hat{A}^{\pm}A = A^{\pm} , \quad \text{and} \quad \hat{A}^{\pm}A^2 = A^{\pm^2} \tag{2-24}$$

These relations can be used to reduce the computational effort in the second- and third-order schemes which are to be described later. For example, we can evaluate $a\hat{A}^{\pm} + bA^{\pm} + cA^{\pm^2}$ as $Q\mathrm{diag}\{a\hat{a}_\ell^{\pm} + ba_\ell^{\pm} + ca_\ell^{\pm^2}\}Q^{-1}$. It is also noted that

$$A^{\pm}\partial_x U = \hat{A}^{\pm}A\partial_x U = \hat{A}^{\pm}\partial_x F \tag{2-25}$$

Symbolically, we can view "$\hat{A}^{\pm} = A^{\pm}/A$," which enables us to convert schemes for quasi-linear hyperbolic equations to schemes for hyperbolic conservation laws very directly and vice versa.

Equations (2-10) and (2-20) are equivalent systems if no transonic shock transitions occur. One needs some information about the propagation speed when transonic shock transition takes place. Equation (2-10) does not have this mechanism, hence shock-fitting (or tracking) is needed. Equation (2-20) allows us to do shock-capturing calculations owing to its conservative property. It is observed that, in general, first-order schemes are adequate for the resolution of shock discontinuities; but for contact discontinuities, higher-order schemes are desirable.

3. ENTROPY SATISFYING SHOCK TRANSITION OPERATORS

The scheme defined by equations (2-20) and (2-22) is suitable for time-dependent calculations. It was observed that, for stationary shock calculation, spikes appear sometimes at the shock transition zones due to violations of the physical domain of dependence. It was also found that scheme (2-20) itself, when applied to the inviscid Bergers' equation, admits stationary expansion shocks (consider $f(u) = u^2/2$ with initial data $u_0 = -1$, $x < 0$, $u_0 = +1$, $x > 0$) and, therefore, is not entropy satisfying.

The Engquist-Osher scheme has a mechanism to provide an entropy satisfying transonic shock transition (spreading over at most two transition cells) through an integration formulation (ref. 9). It was investigation of the scheme of Engquist and Osher which prompted the work of the present section.

It is important to understand what kind of transition path a conservative, shock-capturing, finite difference scheme takes when differencing across a transonic transition zone where the eigenvalue switches sign. Differencing across shock transition zones is necessary for satisfying the Rankine-Hugoniot jump relation and for generating the correct shock speed, hence allowing one to do shock-capturing calculations. Most schemes do not have a special design to handle this transonic shock transition and this transition spreads over several "so-called" transition cells; sometimes this may damage the scheme.

6

In this section, we address this transonic shock transition problem for a conservative upwind difference scheme according to the upwind differencing principle and the entropy conditions.

A shock transition operator is introduced into scheme (2-20) when transonic shock transition is detected. There are two types of transonic shock transitions: (1) transonic shock (where the eigenvalue or characteristic speed changes from positive to negative) and (2) transonic expansion (where the characteristic speed changes from negative to positive) (see fig. 1).

For illustrative purposes, we consider a single conservation law:

$$\partial_t u + \partial_x f(u) = 0 , \quad a(u) = \partial f / \partial u \tag{3-1}$$

Equation (2-20) for (3-1) becomes:

$$\Delta u_j^n = u_j^{n+1} - u_j^n = -\lambda \hat{a}_{j-(1/2)}^+ (f_j^n - f_{j-1}^n) - \lambda \hat{a}_{j+(1/2)}^- (f_{j+1}^n - f_j^n) \tag{3-2}$$

The shock transition operators are applied when shock transition is detected. For example, if the shock transition lies between nodal points J and $J + 1$ (as depicted in fig. 1), i.e.,

$$a_J a_{J+1} < 0 \tag{3-3}$$

We can approximately locate the position of the sonic point, $x^* = (J + \theta)\Delta x$ where $a* = 0$, by the following formula:

$$\theta = -a_J / (a_{J+1} - a_J) \tag{3-4}$$

The state variable $u*$ and the flux vector $f*$ at the sonic point can be approximated by

$$u* = u_J + \theta(u_{J+1} - u_J)$$

and

$$f* = f_J + \theta(f_{J+1} - f_J) \quad \text{or} \quad f* = f(u*)$$

After locating the sonic point, we can separate the interval $[J \Delta x, (J + 1)\Delta x]$ into two parts $[J \Delta x, (J + \theta)\Delta x]$ and $[(J + \theta)\Delta x, (J + 1)\Delta x]$ by the sonic point. In each part the eigenvalue distribution is of the same sign, either positive or negative. Then we can apply upwind differencing according to the sign of the eigenvalue in each region which the flux difference interval covers.

To update the state variable at nodal point J, we use

$$\Delta u_J^n = u_J^{n+1} - u_J^n = -\lambda \hat{a}_{J-(1/2)}^+ (f_J - f_{J-1})$$

$$-\lambda \frac{(\hat{a}_J^- + \hat{a}_*^-)}{2} (f* - f_J) - \lambda \frac{(\hat{a}_*^- + \hat{a}_{J+1}^-)}{2} (f_{J+1} - f*) \tag{3-5a}$$

and to update the state variable at nodal point $J + 1$, we use

$$\Delta u_{J+1}^n = u_{J+1}^{n+1} - u_{J+1}^n = -\lambda \hat{a}_{J+(3/2)}^- (f_{J+2} - f_{J+1})$$

$$-\lambda \frac{(\hat{a}_J^+ + \hat{a}_*^+)}{2} (f* - f_J) - \lambda \frac{(\hat{a}_*^+ + \hat{a}_{J+1}^+)}{2} (f_{J+1} - f*) \qquad (3-5b)$$

In equations (3-5a,b), the split normalized eigenvalues $\hat{a}_*^{\pm}$ need some special treatment in order to be consistent with the upwind differencing. Since the sign function for zero is indeterminate, one way is to use the asymptotic values (0^+) and (0^-). For equation (2-18), we have

$$\text{sgn}(0^+) = 1 \quad \text{and} \quad \text{sgn}(0^-) = -1 \qquad (3-6)$$

To determine the values of $\hat{a}_*^{\pm}$, we take

$$\frac{(\hat{a}_J^{\pm} + \hat{a}_*^{\pm})}{2} \approx \hat{a}_J^{\pm} \qquad (3-7a)$$

and

$$\frac{(\hat{a}_{j+1}^{\pm} + \hat{a}_*^{\pm})}{2} \approx \hat{a}_{J+1}^{\pm} \qquad (3-7b)$$

In so doing, we can avoid entropy-violating transition and the differencing is consistent with the principle of upwind differencing of Courant, Isaacson, and Rees (ref. 1).

For a single conservation law, the scheme defined by equations (3-2), (3-5a), and (3-5b) is identical to the scheme of Engquist and Osher (ref. 9) which is also identical to the flux vector splitting scheme of Steger and Warming (ref. 7). The same procedure can be applied to the systems (2-20). For example, in one-dimensional gas dynamics, the equation corresponding to equation (3-3) is

$$(u - c)_J (u - c)_{J+1} < 0 \qquad (3-8)$$

where u is the fluid velocity and c is the local speed of sound of the fluid.

Numerical examples for a single conservation law, and for systems of hyperbolic conservation laws involving moving shocks, stationary shocks, and transonic expansions are considered and the results are included in a later section.

4. SECOND-ORDER UPWIND DIFFERENCE SCHEMES

In reference 19, Fromm's zero-average-phase-error scheme (ref. 16) for integrating the linear convection equation (2-5) was made monotonic by van Leer through the inclusion of nonlinear feedback terms (or flux limiters). In this section, we will extend van Leer's second-order "monotonicity-preserving" scheme for a single

conservation law to a hyperbolic system of conservation laws in a very natural way through the use of the normalized Jacobian matrix $\hat{A}^{\pm}$ and its associated properties described in section 2.

A second-order accurate TVD scheme using van Leer's (ref. 19) smoothness monitor based on the characteristic flux difference splitting concept can be expressed as follows:

$$
\begin{aligned}
U_j^{n+1} - U_j^n = &-\lambda(\hat{A}^+_{j-(1/2)}\Delta_{j-(1/2)}F + \hat{A}^-_{j+(1/2)}\Delta_{j+(1/2)}F) - \frac{\lambda}{4}(I - S(\theta_j))[(\hat{A}^+_{j+(1/2)} \\
&- \lambda A^+_{j+(1/2)})\Delta_{j+(1/2)}F - (\hat{A}^+_{j-(1/2)} - \lambda A^+_{j-(1/2)})\Delta_{j-(1/2)}F] \\
&- \frac{\lambda}{4}(I + S(\theta_{j-1}))[(\hat{A}^+_{j-(1/2)} - \lambda A^+_{j-(1/2)})\Delta_{j-(1/2)}F - (\hat{A}^+_{j-(3/2)} \\
&- \lambda A^+_{j-(3/2)})\Delta_{j-(3/2)}F] + \frac{\lambda}{4}(I - S(\theta_{j+1}))[(\hat{A}^-_{j+(3/2)} + \lambda A^-_{j+(3/2)})\Delta_{j+(3/2)}F \\
&- (\hat{A}^-_{j+(1/2)} + \lambda A^-_{j+(1/2)})\Delta_{j+(1/2)}F] + \frac{\lambda}{4}(I + S(\theta_j))[(\hat{A}^-_{j+(1/2)} \\
&+ \lambda A^-_{j+(1/2)})\Delta_{j+(1/2)}F - (\hat{A}^-_{j-(1/2)} + \lambda A^-_{j-(1/2)})\Delta_{j-(1/2)}F]
\end{aligned}
\tag{4-1}
$$

Here $S(\theta_j)$ is a diagonal matrix given by

$$
S(\theta_j) = \text{diag}\{s_\ell(\theta_j)\} , \quad \ell = 1, 2, \ldots, m
$$

where

$$
s_\ell(\theta_j) = \begin{cases}
0 , & \text{if} \quad |\Delta_{j+(1/2)}u_\ell| + |\Delta_{j-(1/2)}u_\ell| = 0 \\[2mm]
\dfrac{(|\Delta_{j+(1/2)}u_\ell| - |\Delta_{j-(1/2)}u_\ell|)}{(|\Delta_{j+(1/2)}u_\ell| + |\Delta_{j-(1/2)}u_\ell|)} , & \text{otherwise}
\end{cases}
\tag{4-2}
$$

The so-called "smoothness monitor" θ_j is a quantity that, in some way, measures the rate of change of Δu_ℓ across a nodal point. It is given by

$$
\theta_j = \Delta_{j+(1/2)}u_\ell / \Delta_{j-(1/2)}u_\ell
$$

For a more detailed description on this subject, the reader is encouraged to read the original papers of van Leer (refs. 19,25,26). Without smoothing (i.e., $s_\ell(\theta_j) = 0$), and for the constant coefficient case, equation (4-1) is equivalent to Fromm's scheme and is the simplest upstream-centered scheme of second-order accuracy and may be regarded as the average of the central difference scheme of Lax and Wendroff (ref. 3) and the purely upwind second-order scheme of Warming and Beam (ref. 17). The flux limiter defined by (4-2) is applied to scheme (4-1) exclusively. There are other nonlinear smoothing techniques available such as the ones devised by Harten (ref. 18) and by Roe (ref. 20). In reference 18 Harten has described a recipe of converting a 3-point first-order accurate TVD scheme into a five-point second-order accurate TVD scheme by using a modified flux function. In the following, a second-order TVD scheme

is described using Harten's (ref. 18) modified flux approach and based on equation (2-15).

First, a modified flux vector is defined for a hyperbolic system of conservation laws based on the characteristic flux difference splitting concept. Then, applying our first-order scheme to this modified flux vector, we solve

$$\partial_t U + \hat{A}^M \partial_x F^M = 0 \tag{4-3}$$

where F^M is the modified flux vector and its value at nodal point j is given by

$$F^M_j = F_j + G_j/\lambda \tag{4-4}$$

where F is the original flux vector and G is an additional vector remaining to be defined. The column vector G at nodal point j is $G_j = (g_{1,j}, g_{2,j}, \ldots, g_{m,j})^T$ with its m components given by

$$g_{\ell,j} = s_{\ell,j+(1/2)} \min(|\tilde{g}_{\ell,j+(1/2)}|, |\tilde{g}_{\ell,j-(1/2)}|) \ , \quad \text{when} \quad \tilde{g}_{\ell,j+(1/2)} \tilde{g}_{\ell,j-(1/2)} \geq 0$$

$$= 0 \ , \quad \text{when} \quad \tilde{g}_{\ell,j+(1/2)} \tilde{g}_{\ell,j-(1/2)} \leq 0 \tag{4-5}$$

where $\tilde{g}_{\ell,j+(1/2)}$ $(\ell = 1, 2, \ldots, m)$ are components of the following column vector

$$\tilde{G}_{j+(1/2)} = \lambda \text{sgn} A_{j+(1/2)} \Delta_{j+(1/2)} F/2 - \lambda^2 A_{j+(1/2)} \Delta_{j+(1/2)} F/2 \tag{4-6}$$

and

$$s_{\ell,j+(1/2)} = \text{sgn}(\tilde{g}_{\ell,j+(1/2)}) \tag{4-7}$$

The $\text{sgn} A$ in equation (4-6) is given by

$$\text{sgn} A = Q \text{diag}\{\text{sgn } a_\ell\} Q^{-1} \tag{4-8}$$

and the matrix $\hat{A}^M$ in equation (4-3) is related to A^M which is defined as follows:

$$A^M = Q \text{diag}\{a^M_\ell\} Q^{-1} = \partial F^M/\partial U \tag{4-9}$$

A second-order accurate TVD scheme based on characteristic flux difference splitting for equation (4-3) is

$$U^{n+1}_j - U^n_j = -\lambda(\hat{A}^+_{j-(1/2)} \Delta_{j-(1/2)} F^M - \hat{A}^-_{j+(1/2)} \Delta_{j+(1/2)} F^M) \tag{4-10}$$

In equation (4.10) we have assumed that

$$\hat{A}^{M\pm} \approx \hat{A}^\pm$$

The second-order schemes defined by equations (4-1) and (4-10) are total variation nonincreasing which can be proven (at least for the scalar case; see Sweby, ref. 22).

10

5. THIRD-ORDER UPWIND DIFFERENCE SCHEME

In references 25 and 26, van Leer also investigated third-order schemes for numerical convection based on upstream-centered differencing which is regarded as higher-order sequels to Godunov's method (ref. 6). Before van Leer, Wesseling (ref. 27) derived and tested various high-order upstream schemes, among which are Fromm's (ref. 16) scheme, and the third-order scheme. His tests also include several central difference schemes, among which are the Lax-Wendroff (ref. 3) scheme and the third-order (RBM) scheme derived by Rusanov (ref. 28) and by Burstein and Mirin (ref. 29). It is well known that for five-point two time-level upwind schemes the highest order which can be achieved is three. It is also found that third-order schemes have less dispersion error than the second-order schemes (refs. 26 and 30). Thus it is interesting to see how much can be gained in going to third-order accuracy.

In this section, we describe a third-order upwind (or upstream-centered) scheme for integrating hyperbolic systems of conservation laws by applying our characteristic flux difference splitting concept to a third-order upstream-centered scheme for the linear wave equation (eq. (35) of ref. 25). The procedure is similar to the one we described previously for the second-order scheme using van Leer's flux limiter (ref. 9).

By using the peculiar properties (eq. (2-24)) of the normalized Jacobian matrices $\hat{A}^{\pm}$ and the Jacobian matrices $A^{\pm}$ of a hyperbolic system of conservation laws, a third-order accurate upwind (upstream-centered) difference scheme for integrating equation (2-15) can be expressed as follows:

$$
\begin{aligned}
U_j^{n+1} - U_j^n = &-\lambda(\hat{A}^+_{j-(1/2)}\Delta_{j-(1/2)}F + \hat{A}^-_{j+(1/2)}\Delta_{j+(1/2)}F) - \frac{\lambda}{6}(I - S(\theta_j))[2\hat{A}^+_{j+(1/2)} \\
&- 3\lambda A^+_{j+(1/2)} + \lambda^2 A^{+2}_{j+(1/2)}\Delta_{j+(1/2)}F - (2\hat{A}^+_{j-(1/2)} - 3\lambda A^+_{j-(1/2)} \\
&+ \lambda^2 A^{+2}_{j-(1/2)})\Delta_{j-(1/2)}F] - \frac{\lambda}{6}(I + S(\theta_{j-1}))[(\hat{A}^+_{j-(1/2)} - \lambda^2 A^{+2}_{j-(1/2)})\Delta_{j-(1/2)}F \\
&- (\hat{A}^+_{j-(3/2)} - \lambda^2 A^{+2}_{j-(3/2)})\Delta_{j-(3/2)}F] + \frac{\lambda}{6}(I - S(\theta_{j+1}))[(\hat{A}^-_{j+(3/2)} \\
&- \lambda^2 A^{-2}_{j+(3/2)}\Delta_{j+(3/2)}F - (\hat{A}^-_{j+(1/2)} - \lambda^2 A^{-2}_{j+(1/2)})\Delta_{j+(1/2)}F] \\
&+ \frac{\lambda}{6}(I + S(\theta_j))[(2\hat{A}^-_{j+(1/2)} + 3\lambda A^-_{j+(1/2)} + \lambda^2 A^{-2}_{j+(1/2)})\Delta_{j+(1/2)}F \\
&- (2\hat{A}^-_{j-(1/2)} + 3\lambda A^-_{j-(1/2)} + \lambda^2 A^{-2}_{j-(1/2)})\Delta_{j-(1/2)}F]
\end{aligned}
\tag{5-1}
$$

where $S(\theta_j)$ is defined as in equation (4-2). Note that all members of equation (5-1) are perfect differences; hence, the scheme is conservative. Whether the scheme defined by equation (5-1) is TVD or not is yet to be proven. But the flux limiters for the present third-order scheme seems to work remarkably well for one-dimensional problems; numerical results indicate the scheme is monotonicity-preserving. Dispersive and dissipative properties and the global order of accuracy of this third-order scheme will be examined in the following section. In this report, the third-order

11

scheme (5-1) is currently limited to one-dimensional problems only. Present knowledge of nonlinear smoothing techniques for third- and higher-order schemes is rather limited, and further study of this is warranted (refs. 26 and 31).

A linear stability analysis, assuming $A = $ constant, yields the following stability bound for scheme (5-1):

$$|A|\lambda \le 1 \qquad (5-2)$$

Equation (5-2) is also the stability bound for the second-order schemes equations (4-1) and (4-10).

6. STABILITY AND ACCURACY OF THE SECOND- AND THIRD-ORDER SCHEMES

To perform a linear stability analysis, the second-order scheme equation (4-1) and the third-order scheme equation (5-1) are applied to the linear wave equation (2-5) which is the model equation for the hyperbolic system equation (2-2).

We rewrite equation (2-5) as

$$\partial_t u + a\partial_x u = 0 \qquad (6-1)$$

A general expression for explicit two time-level difference schemes which approximate equation (6-1) is

$$u_j^{n+1} = \sum_{k_1}^{k_2} c_k u_{j+k}^n \qquad (6-2)$$

With a assumed constant, the amplification factor g of equation (6-1) is defined in the customary way as the ratio of the amplitudes of a harmonic wave $u(x,t) = u(t)\exp(i\nu x)$ at time $t + \Delta t$ and time t. Thus one finds:

$$g(\theta) = \exp(-i\sigma\theta) \qquad (6-3)$$

where $\sigma = \lambda a$ is the Courant number, and $\theta = \nu\Delta x$.

Equation (6-3) has unit modulus and a phase shift per time increment Δt of

$$\phi_e = -a\nu\Delta t = -\sigma\theta \qquad (6-4)$$

The amplification factor g_h of the difference scheme equation (6-2) is found to be:

$$g_h(\theta) = \sum_{k_1}^{k_2} c_k \exp(ik\theta) \qquad (6-5)$$

For scheme equation (4-1), it is found that the coefficients c_k are given by

$$c_{-2} = -\lambda a^+(1 - \lambda a^+)/4 \qquad (6-6a)$$

$$c_{-1} = \lambda a^+ + \lambda a(1 - \lambda|a|)/4 \qquad (6\text{-}6b)$$

$$c_0 = 1 - 3\lambda|a|/4 - \lambda^2 a^2/4 \qquad (6\text{-}6c)$$

$$c_{+1} = -\lambda a^- - \lambda a(1 - \lambda|a|)/4 \qquad (6\text{-}6d)$$

$$c_{+2} = \lambda a^-(1 + \lambda a^-)/4 \qquad (6\text{-}6e)$$

With these coefficients and equation (6-2), it is easy to find that the Taylor exapnsion of the scheme is

$$\Delta u_j^n = u_j^{n+1} - u_j^n = -\lambda a \Delta x (\partial_x u)_j + \frac{1}{2}(\lambda a \Delta x)^2(\partial_{xx} u)_j$$

$$+ (\lambda a \Delta x^3/12 - \lambda^2 \Delta x^2 a|a|)(\partial_{xxx} u)_j \qquad (6\text{-}7)$$

which is of second-order accuracy both in time and space.

The amplification factor for the second-order scheme is

$$g_h(\theta) = \text{Re } g_h(\theta) + i \text{ Im } g_h(\theta) = 1 - |\sigma|(1 - \cos\theta)[1 + |\sigma| - (1 - |\sigma|)\cos\theta]/2$$

$$- i\sigma \sin\theta[3 - |\sigma| - (1 - |\sigma|)\cos\theta]/2 \qquad (6\text{-}8)$$

The phase shift ϕ per time step of the finite-difference scheme can be computed by the formula

$$\phi = \sin^{-1}\{\text{Im } g_h(\theta)/|g_h|\} \qquad (6\text{-}9)$$

The relative phase error of scheme (4-1) is given by the ratio of (6-9) and (6-4).

Dissipative (amplitude distortion) and dispersive (phase shift) errors can be conveniently represented as polar plots of $|g_h(\theta)|$ and ϕ/ϕ_e, as a function of θ.

The same procedure can be carried out for the third-order scheme (5-1).

The coefficients c_k for (5-1) are given by

$$c_{-2} = -\lambda a^+(1 - \lambda^2(a^+)^2)/6 \qquad (6\text{-}10a)$$

$$c_{-1} = \lambda|a|(1 - \lambda^2 a^2)/3 + \lambda a(1 + \lambda a)(4 - \lambda a)/6 \qquad (6\text{-}10b)$$

$$c_0 = (1 - \lambda|a|/2)(1 - \lambda^2 a^2) \qquad (6\text{-}10c)$$

$$c_{+1} = \lambda|a|(1 - \lambda^2 a^2)/3 - \lambda a(1 - \lambda a)(4 + \lambda a)/6 \qquad (6\text{-}10d)$$

$$c_{+2} = \lambda a^-(1 - \lambda^2(a^-)^2)/6 \qquad (6\text{-}10e)$$

The Taylor expansion for equation (6-2) with (6-10) is

13

$$\Delta u_j^n = u_j^{n+1} - u_j^n = -\lambda a \Delta x (\partial_x u)_j + \frac{1}{2} (\lambda a \Delta x)^2 (\partial_{xx} u)_j - \frac{1}{6} (\lambda a \Delta x)^3 (\partial_{xxx} u)_j$$

$$- \frac{1}{12} \lambda |a| (1 - \lambda |a|/2 - \lambda^2 a |a|) \Delta x^4 (\partial_{xxxx} u)_j \tag{6-11}$$

The accuracy of this scheme is third-order in time and space.

The amplification factor for the third-order scheme is given by

$$g_h(\theta) = 1 - |\sigma|(1 - \cos \theta)[1 + 3|\sigma| - \sigma^2 - (1 - |\sigma|^2)\cos \theta]/3$$

$$+ i\sigma \sin \theta [(1 - \sigma^2)\cos \theta - (4 - \sigma^2)]/3 \tag{6-12}$$

The dissipation and dispersion of (6-12) can be similarly computed.

Figure 2 shows plots of the amplification factor modulus and phase error of the second- and third-order schemes for several values of the Courant number σ in the stable range.

In terms of dissipation, the third-order scheme is slightly less dissipative than the second-order scheme. But also, in terms of disperson, the third-order scheme has a larger dispersion.

In order to check the global order of accuracy of the second-order and the third-order schemes, we next describe some numerical experiments with periodic scalar conservation law

$$\partial_t u + \partial_x (u^2/2) = 0 \qquad -\pi \le x \le \pi, t \ge 0 \tag{6-13a}$$

with initial data

$$u(x,0) = 2 + \sin x ; \qquad -\pi \le x \le \pi \tag{6-13b}$$

and the periodic boundary condition

$$u(-\pi,t) = u(\pi,t) , \qquad t \ge 0 \tag{6-13c}$$

It is easy to see that the solution to equation (6-13) is smooth up to $t = 1$, at which time a shock is formed (see ref. 32 for a more detailed description). The relative L_2-errors are computed at the same physical time for the second-order schemes (4-1) and (4-10) and the third-order scheme (5-1).

In table 1 we present a mesh refinement chart for the schemes defined by (4-1), (4-10), and (5-1). For comparison purposes, we also list the results obtained by using the central difference scheme of Lax and Wendroff (LW) (ref. 3), and the second-order purely upwind difference scheme of Warming and Beam (WB) (ref. 17). The second-order scheme (4-1) without flux limiter, denoted by (II), is identical to the zero-average phase-error scheme of Fromm (F) (ref. 16). (II-a) denotes the second-order TVD scheme with van Leer's flux limiter equation (4-1). The scheme using Harten's (ref. 18) modified flux defined by equation (4-10) is denoted by (II-b). The third-order schemes defined by equation (5-1) without and with flux limiters are represented by (III) and (III-a), respectively.

14

The values Δx and Δt in table 1 are defined by

$$\Delta x = 2\pi/M , \quad \Delta t = 0.95\Delta x/3$$

The relative L_2-error in this chart correspond to results at $t = 0.497$, at which the solution is still smooth. The relative L_2-error used in table 1 is defined by

$$\sqrt{\Delta x \sum_j (u_j - v_j)^2}$$

where u_j is the numerical solution and v_j is the exact solution obtained by Newton-Raphson iteration.

From the data of the numerical experiments in table 1, we observe that the second- and third-order schemes without flux limiters (II and III) are fully second- and third-order accurate; a refinement by a factor of 2 reduces the error by a factor of approximately $4 = 2^2$ and $8 = 2^3$, respectively. With flux limiters, the second- and third-order schemes have about the same quality of results; the global order of accuracy for both schemes is around 3/2. In general, the upstream-centered difference schemes (II-a and III-a) demonstrate more accurate than the central difference schemes (LW and II-b).

7. THE EULER EQUATIONS OF INVISCID GAS DYNAMICS

In this section, we apply the above development to the Euler equations of inviscid gas dynamics in one and two space dimensions. The one-dimensional Euler equations can be written in conservation-law form as

$$\partial_t U + \partial_x F(U) = 0 \tag{7-1}$$

where $U = (\rho,\rho u,e)^T$ is the state vector of conservative variables and $F = (\rho u,\rho u^2 + p,(e + p)u)^T$ is the flux vector. The so-called primitive variables of equation (7-1) are the fluid density ρ, the velocity u, and the pressure p. For a perfect gas, the total energy per unit volume, e, is related to the other variables by $e = p/(\gamma - 1) + 0.5\,\rho u^2$, where γ is the ratio of the specific heats. Equation (7-1) can be expressed in nonconservative quasi-linear form as

$$\partial_t U + A\partial_x U = 0 \tag{7-2}$$

where A is the Jacobian matrix $\partial F/\partial U$

$$\begin{bmatrix} 0 & 1 & 0 \\ (\gamma - 3)u^2/2 & (3-\gamma)u & (\gamma - 1) \\ (\gamma - 1)u^3 - \gamma eu/\rho & \gamma e/\rho - 3(\gamma - 1)u^2/2 & \gamma u \end{bmatrix} \tag{7-3}$$

The eigenvalues of A are

$$a_1 = u , \quad a_2 = u + c , \quad \text{and} \quad a_3 = u - c \tag{7-4}$$

15

where $c = \sqrt{\gamma p/\rho}$ is the local speed of sound. The coefficient matrix A can be diagonalized by the similarity transformation matrix $Q = MT$ with M and T given by

$$M = \partial U/\partial \tilde{U} = \begin{bmatrix} 1 & 0 & 0 \\ u & \rho & 0 \\ u^2/2 & \rho u & 1/(\gamma - 1) \end{bmatrix} \qquad (7\text{-}5)$$

$$T = \begin{bmatrix} 1 & \rho/2c & -\rho/2c \\ 0 & 1/2 & 1/2 \\ 0 & \rho c/2 & -\rho c/2 \end{bmatrix} \qquad (7\text{-}6)$$

where $\tilde{U} = (\rho, u, p)^T$. M^{-1} and T^{-1} are the inverse matrices of M and T and can be easily obtained.

We have

$$\Lambda = T^{-1}M^{-1}AMT = \begin{bmatrix} u & 0 & 0 \\ 0 & u+c & 0 \\ 0 & 0 & u-c \end{bmatrix} \qquad (7\text{-}7)$$

The matrix A is split into two parts as

$$A = A^+ + A^- = MT(\Lambda^+ + \Lambda^-)T^{-1}M^{-1} \qquad (7\text{-}8)$$

Similarly, we have

$$\hat{A} = \hat{A}^+ + \hat{A}^- = MT(\hat{\Lambda}^+ + \hat{\Lambda}^-)T^{-1}M^{-1} = I \qquad (7\text{-}9)$$

As indicated in equation (2-22) we can also evaluate $\hat{A}^{\pm}_{j-(1/2)}$ as

$$\hat{A}^{\pm}_{j-(1/2)} = \bar{M}\bar{T}\hat{\bar{\Lambda}}^{\pm}\bar{T}^{-1}\bar{M}^{-1} \qquad (7\text{-}10)$$

where $\bar{M}$ and $\bar{T}$ are given by

$$\bar{M} = \begin{bmatrix} 1 & 0 & 0 \\ \bar{u} & \bar{\rho} & 0 \\ (\bar{u})^2/2 & \bar{\rho}\bar{u} & 1/(\gamma - 1) \end{bmatrix} \qquad (7\text{-}11)$$

and

$$\bar{T} = \begin{bmatrix} 1 & \bar{\rho}/(2\bar{c}) & -\bar{\rho}/(2\bar{c}) \\ 0 & 1/2 & 1/2 \\ 0 & \bar{\rho}\bar{c}/2 & -\bar{\rho}\bar{c}/2 \end{bmatrix} \qquad (7\text{-}12)$$

16

The overbar quantities are evaluated by a two-point average.

For example, $(\bar{u})_{j-(1/2)}$ is defined as $(u_{j-1} + u_j)/2$. For the Euler equations in multiple space dimensions, similar procedures can be applied; below we briefly describe some of the highlights. Details of the formulation for the three-dimensional Euler equations in general curvilinear coordinates can be found in reference 14.

The unsteady two-dimensional Euler equations in conservation-law form are given by

$$\partial_t U + \partial_x F + \partial_y G = 0 \tag{7-13}$$

where $U = (\rho, \rho u, \rho v, e)^T$, $F = (\rho u, \rho u^2 + p, \rho uv, (e + p)u)^T$, and $G = (\rho v, \rho vu, \rho v^2 + p, (e + p)v)^T$.

In the above equation ρ is the density, u and v the velocity components corresponding to the x and y coordinates, e the total internal energy per unit volume, p the pressure, and γ the specific heat ratio.

The equation of state is

$$p = (\gamma - 1)\left[e - \frac{1}{2}\rho(u^2 + v^2)\right]$$

Applying the characteristic flux difference splitting method to equation (7-13) we have

$$\partial_t U + (\hat{A}^+ + \hat{A}^-)\partial_x F + (\hat{B}^+ + \hat{B}^-)\partial_y G = 0 \tag{7-14}$$

where

$$\hat{A}^{\pm} = MT_x \hat{\Lambda}_x^{\pm} T_x^{-1} M^{-1} \quad \text{and} \quad \hat{B}^{\pm} = MT_y \hat{\Lambda}_y^{1} T_y^{-1} M^{-1} \tag{7-15}$$

Matrices $\bar{M}$, $\bar{T}_x^{-1}$, and $\bar{T}_y^{-1}$ are given by

$$\bar{M}^{-1} = \begin{bmatrix} 1 & 0 & 0 & 0 \\ -\bar{u}/\bar{\rho} & 1/\bar{\rho} & 0 & 0 \\ -\bar{v}/\bar{\rho} & 0 & 1/\bar{\rho} & 0 \\ (\gamma - 1)(\bar{u}^2 + \bar{v}^2)/2 & -(\gamma - 1)\bar{u} & -(\gamma - 1)\bar{v} & (\gamma - 1) \end{bmatrix} \tag{7-16}$$

$$\bar{T}_x^{-1} = \begin{bmatrix} 1 & 0 & 0 & -1/(\bar{c})^2 \\ 0 & \bar{\rho} & 0 & 1/\bar{c} \\ 0 & 0 & 1 & 0 \\ 0 & \bar{\rho} & 0 & -1/\bar{c} \end{bmatrix} \tag{7-17}$$

and

$$\bar{T}_y^{-1} = \begin{bmatrix} 1 & 0 & 0 & 1/(\bar{c})^2 \\ 0 & 1 & 0 & 0 \\ 0 & 0 & \bar{\rho} & 1/\bar{c} \\ 0 & 0 & \bar{\rho} & -1/\bar{c} \end{bmatrix} \qquad (7\text{-}18)$$

A second-order scheme using van Leer's (ref. 19) flux limiter can be constructed as in the one-dimensional case, applying the same flux difference components for F to the flux vector G and simply replacing the A's by the matrices B's. Numerical experiments for two-dimensional Euler equations using this scheme have been reported in reference 12.

Similarly, we can apply Harten's (ref. 8) modified flux to solve

$$\partial_t U + (\hat{A}^+ + \hat{A}^-)\partial_x F^M + (\hat{B}^+ + \hat{B}^-)\partial_y G^M = 0 \qquad (7\text{-}19)$$

The modified flux in the x direction F^M is defined in the same manner as in Section 4. The modified flux in the y direction G^M can be similarly defined.

An explicit second-order TVD scheme based on equation (7-19) can be expressed as

$$U_{j,k}^{n+1} - U_{j,k}^n = -\lambda[\hat{A}_{j-(1/2),k}^+(F_{j,k}^M - F_{j-1,k}^M) + \hat{A}_{j+(1/2),k}^-(F_{j+1,k}^M - F_{j,k}^M)]$$

$$- \lambda[\hat{B}_{j,k-(1/2)}^+(G_{j,k}^M - G_{j,k-1}^M) + \hat{B}_{j,k+(1/2)}^-(G_{j,k+1}^M - G_{j,k}^M)] \quad (7\text{-}20)$$

For implicit schemes, Strang-type dimensional splitting can be applied to construct robust schemes as described in reference 14.

For flow problems involving complex geometry, the above development for the Euler equations in Cartesian coordinates can be easily extended to general curvilinear coordinates. For a multidimensional case, the third-order scheme with the flux limiter defined by equation (4-2) is not sufficient to make the scheme stable, further study on the flux limiter (nonlinear filtering techniques) for higher order "monotonic" upwind schemes is needed (ref. 31).

8. RESULTS AND DISCUSSIONS

In this section, we present the results of some numerical experiments using the second- and third-order upwind difference schemes which we have described previously. Single conservation laws and systems are considered. For single equations, we consider the inviscid Burgers' equation, and, for systems of equations, the Euler equations of inviscid gas dynamics in one and two space dimensions are considered. For third-order schemes, only results for one-dimensional problems are presented. For all the following numerical calculations, uniform computational mesh systems are employed.

18

(a) Inviscid Burgers' Equation

The first model problem we consider is the inviscid Burgers' equation.

$$\partial_t u + \partial_x f(u) = 0 , \quad f(u) = u^2/2$$

with initial conditions

$$u(x < 0) = u_L , \quad \text{and} \quad u(x > 0) = u_R$$

The u_L and u_R values can be chosen to represent different situations which may occur in transonic aerodynamics. We consider the following four cases:

(a) transonic moving shock: $u_L = 2, \quad u_R = -1$

(b) transonic stationary shock: $u_L = 1, \quad u_R = -1$

(c) transonic expansion: $u_L = -1, \quad u_R = 1$

(d) fully supersonic: $u_L = 0.5, \quad u_R = 1$

The following initial values were prescribed

$$u_j = u_L \quad \text{for} \quad j < J$$

$$u_j = u_R \quad \text{for} \quad j \geq J + 1$$

For cases (a-c), J is equal to 25 and for case (d) J is 16. The total number of mesh points is 50 and the mesh size is $\Delta x = 0.01$. Figures 3(a)-3(c) display the solutions using scheme (2-5a,b) for cases (a-c). Transonic moving and stationary shocks are captured within two zones and the transonic expansion shock is excluded.

Figures 4(a) and 4(b) show results for case (c) using the second- and third-order accurate schemes.

For case (d), we solve the case as reported by van Leer in reference 19 for comparison purposes. Figures 5(a)-5(d) show the second- and third-order results without and with nonlinear smoothing, respectively.

In order to further test the present method we also include the solution to equation (6-13) at two instants; one at time $t = 0.497$, at which the solution is still smooth and another at time $t = 0.995$, at which time a shock is formed. Figures 6(a), 6(b), 7(a), and 7(b) show the results using the second-and third-order schemes (II, IIa, III, and IIIa) with 20 grid points ($M = 20$ in table 1).

(b) Ideal Shock Tube Problem (One-Dimensional Euler Equations)

We consider the ideal shock tube problem as our second model problem for the one-dimensional Euler equations. The case we consider here is the one reported by Sod (ref. 27). The initial conditions defined in the problem are

$$p_L = 1 \quad , \quad \rho_L = 1 \quad , \quad u_L = 0 \quad , \quad 0 < x < 0.5$$

$$p_R = 0.1 \quad , \quad \rho_R = 0.125 \quad , \quad u_R = 0 \quad , \quad 0.5 < x < 1$$

The space-step size Δx used is 0.01. The time step Δt is calculated at each time level subject to the condition that the maximum Courant number is 0.9, and the output is at time $t = 0.24$. The velocity, density, pressure, internal energy, and entropy profiles are presented for all calculations. The numerical solution (box with connecting line, every other point) and the exact solution (solid line) are plotted.

Figures 8(a)-8(e) indicate the results using scheme equation (4-1) without flux limiters (II). Figures 9(a)-9(e) show the results using scheme (4-1) with flux limiters (IIa). These results have been reported in reference 14 and are comparable to those reported by van Leer using his MUSCL scheme (ref. 34). The MUSCL scheme is a Lagrangean scheme, and the Lagrangean results are remapped with least-squares accuracy onto the desired Euler grid in a separate step. The present scheme (IIa) can be viewed as the corresponding Eulerian scheme for MUSCL scheme.

Figures 10(a)-10(e) display the results using equation (4-10) with Harten's (ref. 18) modified flux (IIb). These results invite comparison with those obtained using Harten's high resolution scheme (ref. 18).

Figures 11(a)-11(e) show the third-order results using scheme equation (5-1) with van Leer's (ref. 19) flux limiters (IIIa).

It is observed that the shock profile is sharpened compared with second-order results. For the contact surface profiles, the one using van Leer's (ref. 19) flux limiter is slightly less smeared than that using Harten's (ref. 23) modified flux.

To appreciate the effect of flux limiters, the third-order results without flux limiters (III) are also shown in figures 12(a)-12(e). The flux limiters defined by equation (4-2) seem to work very well in this one-dimensional problem.

(c) Quasi-One-Dimensional Nozzle Problem

The nozzle geometry we consider here is a divergent nozzle with area distribution

$$A(x) = 1.398 + 0.347 \tanh(0.8 x - 4) \quad , \quad 0 \le x \le 10$$

We consider the case of supersonic inflow and subsonic outflow with a stationary shock. For all explicit schemes, we use $CFL = 0.9$. Uniform mesh distribution with mesh size $\Delta x = 0.2$ (50 grid points) is used. The converged solution is obtained in about 800 iterations (with maximum residual less than 10^{-6}). The density and mass-flux distributions are plotted.

Figures 13(a), 13(b), 14(a), and 14(b) show results using the first-order explicit scheme and averages defined by equation (2-22) without and with transonic shock operators, respectively. We can see that the spike which appears near the post-shock region in figure 13 has been eliminated in figure 14.

In figures 15(a) and 15(b), we show the corresponding results using the first-order implicit scheme with averages defined by equation (2-23) and $CFL = 25$.

Both figures 14 and 15 display a clean shock profile which occupies one mesh interval.

In figures 16 and 17, we show results using the second-order explicit schemes (IIa) and (IIb), respectively. Comparing with the first-order results, the second-order effect can be seen from the mass-flux profile near the post-shock region.

For steady shock calculations, we found that there is no need to apply transonic shock operators if one uses the averages defined by equation (2-23) (here eqs. (7-10) to (7-12)). This type of average, in general, captures steady-state shocks within one transition cell as also observed by other approaches (refs. 11 and 8).

In figures 18(b) and 18(b), we present the results using the third-order scheme equation (5-1).

(d) Plane Shock Reflection (Two-Dimensional Euler Equations)

In order to test the current characteristic flux difference splitting method in a multidimensional problem, we consider the plane shock reflection problem. Here a simple regular reflection and a Mach reflection are considered. Preliminary results using second-order schemes only are presented. For the case of regular reflection shock, we solve the case reported by Yee et al. [24]. The incident shock angle is 29° and the free stream Mach number is 2.9. The computational domain is $0 < x < 4$, and $-0 < y < 1$, with uniform grid size of 61*22.

Figure 19(a) and (b) show the density contour and the pressure distribution at $y = 0.5$ using scheme IIa. Figures 20(a) and (b) show the same results using scheme IIb. For the case of simple Mach reflection, the incident shock angle is 42° and the free-stream Mach number is 4.23. The computational grid is 34 by 48 with $\Delta x = \Delta y = 0.1$. Density and pressure contours are shown to demonstrate the resolution and the physical structures as well. Figures 21(a) and (b) show the results using scheme equation (7-19) with Harten's (ref. 23) modified flux approach. The results using the implicit version of scheme (4-1) were reported in reference 12. Further tests and results for more complex flow problems using generalized coordinate systems will be reported in a future study.

9. CONCLUSIONS

In this study, we have described second- and third-order two time-level and five-point upwind difference schemes for hyperbolic systems of conservation laws and their application to the Euler equations of inviscid gas dynamics. Entropy-satisfying transonic shock transition operators are introduced at the sonic point in accord with the principle of upwind differencing which enable the schemes to exclude nonphysical expansion shocks. Stability and accuracy of the second- and third-order schemes are examined. Nonlinear smoothing techniques devised by van Leer (ref. 19) and by Harten (ref. 23) are adapted and generalized to the present framework of characteristic flux difference splitting to make the schemes total variation diminishing (at least for a scalar equation). Numerical experiments also justified this claim. The method offers some simplicity in terms of the mathematical formulations and its accordance with the idea of preserving the physical domain of dependence, hence is adequate for the numerical solution of partial differential equations governing convection (ref. 35).

For the second-order schemes, our results are comparable with those obtained by using van Leer's (ref. 19) and Harten's (ref. 23) high resolution schemes. The third-order scheme, although only tested for one-dimensional problems, displays slightly superior resolution compared with second-order results. Whether or not the present third-order scheme is TVD is yet to be proven; but the results seem to indicate that the scheme is monotonicity-preserving. Further study on higher-order flux limiters for integrating convective-type equations is suggested.

REFERENCES

1. Courant, R.; Isaacson, E.; and Rees, M.: On the Solution of Nonlinear Hyperbolic Differential Equations by Finite Difference. Comm. Pure and Appl. Math., vol. V, 1952, pp. 243-255.

2. Moretti, G.: The λ-Scheme. Computers and Fluids, vol. 7, 1979, pp. 191-205.

3. Lax, P. D.; and Wendroff, B.: Systems of Conservation Laws. Comm. Pure and Appl. Math., vol. 13, 1960, pp. 217-237.

4. MacCormack, R. W.: The Effect of Viscosity on Hyper-velocity Impact Cratering. AIAA Paper 69-354, 1969.

5. Beam, R. M.; and Warming, R. F.: An Implicit Finite-Difference Algorithm for Hyperbolic System in Conservation-Law Form. J. Comp. Phys., vol. 22, 1976, pp. 87-110.

6. Godunov, S. K.: A Difference Scheme for Numerical Computation of Discontinuous Solution of Hydrodynamic Equations. Mat-Sornik 47, 1959.

7. Steger, J.; and Warming, R. F.: Flux Vector Splitting of Inviscid Gasdynamic Equations with Applications to Finite Difference Methods. NASA TM-78605, 1979.

8. Roe, R. P.: The Use of the Riemann Problem in Finite-Difference Schemes. 7th International Numerical Methods in Fluid Dynamics, Lecture Notes in Physics, vol. 141, 1981, pp. 354-359.

9. Engquist, B.; and Osher, S.: One-Sided Difference Approximations for Nonlinear Conservation Laws. Math. Comp., vol. 36, 1981, pp. 321-351.

10. Osher, S.; and Solomon, F.: Upwind Difference Schemes for Hyperbolic Systems of Conservation Laws. Math. Comp., vol. 38, 1982, pp. 339-377.

11. Huang, L. C.: Pseudo-Unsteady Difference Schemes for Discontinuous Solutions of Steady-State One-Dimensional Fluid Dynamics Problems. J. Comp. Phys., vol. 42, 1981, pp. 195-211.

12. Lombard, C. K.; Oliger, J.; and Yang, J. Y.: A Natural Conservative Flux Difference Splitting for the Hyperbolic Systems of Gasdynamics. Presented at the Eighth International Conference on Numerical Methods in Fluid Dynamics, Aachen, West Germany, 1982.

13. Harten, A.; Lax, P.; and van Leer, B.: Upstream Differencing and Godunov-Type Schemes for Hyperbolic Conservation Laws. SIAM Review, vol. 25, 1983. pp. 35-61.

14. Yang, J. Y.: A Characteristic Flux Difference Splitting Method for Hyperbolic Systems of Conservation Laws. Ph.D. Thesis, Stanford University, 1982.

15. Yang, J. Y.; Lombard, C. K.; and Bershader, D.: A Characteristic Flux Difference Splitting for the Hyperbolic Conservation Laws of Inviscid Gasdynamics. AIAA Paper 83-0040, 1983.

16. Fromm, J. E.: A Method for Reducing Dispersion in Convective Difference Schemes. J. Comp. Phys. vol. 3, 1968, pp. 176-189.

17. Warming, R. F.; and Beam, R. M.: Upwind Second Order Difference Schemes and Applications in Aerodynamics. AIAA J., vol. 14, 1976, pp. 1241-1249.

18. Harten, A.: High Resolution Schemes for Hyperbolic Conservation Laws. J. Comp. Phys., vol. 49, 1983, pp. 357-393.

19. van Leer, B.: Towards the Ultimate Conservative Difference Scheme. II. Monotonicity and Conservation Combined in a Second-Order Scheme. J. Comp. Phys., vol. 14, 1974, pp. 361-370.

20. Roe, P. L.: Numerical Algorithms for the Linear Wave Equation. Royal Aircraft Establishment Technical Report 81047, 1981.

21. Chakravarthy, S.; and Osher, S.: High Resolution Applications of the Osher Upwind Scheme for the Euler Equations. AIAA Paper 83-1943, 1983.

22. Sweby, P.: High Resolution Schemes Using Flux Limiters for Hyperbolic Conservation Laws. UCLA Preprint, 1983.

23. Harten, A.: On a Class of High Resolution Total-Variation-Stable Finite-Difference Schemes. NYU Report, October 1982.

24. Yee, H.; Warming, R. F.; and Harten, A.: Implicit Total Variation Diminishing (TVD) Schemes for Steady-State Calculations. AIAA Paper 83-1902, 1983.

25. van Leer, B.: Towards the Ultimate Conservative Difference Scheme. III. Upstream-Centered Finite-Difference Schemes for Ideal Compressible Flow. J. Comp. Phys., vol. 23, 1977, pp. 263-275.

26. van Leer, B.: Towards the Ultimate Conservative Difference Scheme. IV. A New Approach of Numerical Convection. J. Comp. Phys., vol. 23, 1977, pp. 276-299.

27. Wesseling, P.: On the Construction of Accurate Difference Schemes for Hyperbolic Partial Differential Equations. J. Engineering Math, vol. 7, no. 1, 1973.

28. Rusanov, V. V.: On Difference Schemes of Third Order Accuracy for Nonlinear Hyperbolic Systems. J. Comp. Phys., vol. 5, 1970, pp. 507-516.

29. Burstein, S. Z.; and Mirin, A. A.: Third Order Difference Methods for Hyperbolic Equations. J. Comp. Phys., vol. 5, 1970, pp. 547-571.

30. Warming, R. F.; Kutler, P.; and Lomax, H.: Second- and Third-Order Noncentered Difference Schemes for Nonlinear Hyperbolic Equations. AIAA J., vol. 11, no. 2, 1973, pp. 189-196.

31. Forester, C. K.: Higher Order Monotonic Convective Difference Schemes. J. Comp. Phys., vol. 23, no. 1, 1977, pp. 1-22.

32. Harten, A.; and Tal-Ezer, H.: On a Fourth Order Accurate Implicit Finite Differ-
     ence Scheme for Hyperbolic Conservation Laws: I. Non-Stiff Strongly Dynamic
     Problems. ICASE Report no. 79-1, Jan. 1979.

33. Sod, G. A.: Survey of Several Finite Difference Methods for Systems of Nonlinear
     Hyperbolic Conservation Laws," J. Comp. Phys., vol. 27, 1978, pp. 1-31.

34. van Leer, B.: Towards the Ultimate Conservative Difference Scheme. V. A Second-
     Order Sequel to Godunov's Method. J. Comp. Phys., vol. 32, 1979, pp. 101-136.

35. Lomax, H.; Kutler, P.; and Fuller, F. B.: The Numerical Solution of Partial
     Differential Equations Governing Convection. AGARD-AG-146-70, 1970.

TABLE 1.- COMPARISON OF L_2-ERROR FOR SECOND- AND THIRD-ORDER SCHEMES

Δx	LW	WB	F (or II)	II-b	II-a	III	III-a
$\dfrac{2\pi}{20}$	0.449E-01	0.380E-01	0.217E-01	0.295E-01	0.204E-01	0.144E-01	0.166E-01
$\dfrac{2\pi}{40}$	.128E-01	.111E-01	.488E-01	.943E-02	.620E-02	.241E-02	.543E-02
$\dfrac{2\pi}{80}$	.338E-02	.294E-02	.104E-02	.308E-02	.177E-02	.338E-03	.174E-02
$\dfrac{2\pi}{160}$	.863E-03	.754E-03	.230E-03	.973E-03	.503E-03	.442E-04	.534E-03

(a)   (b)
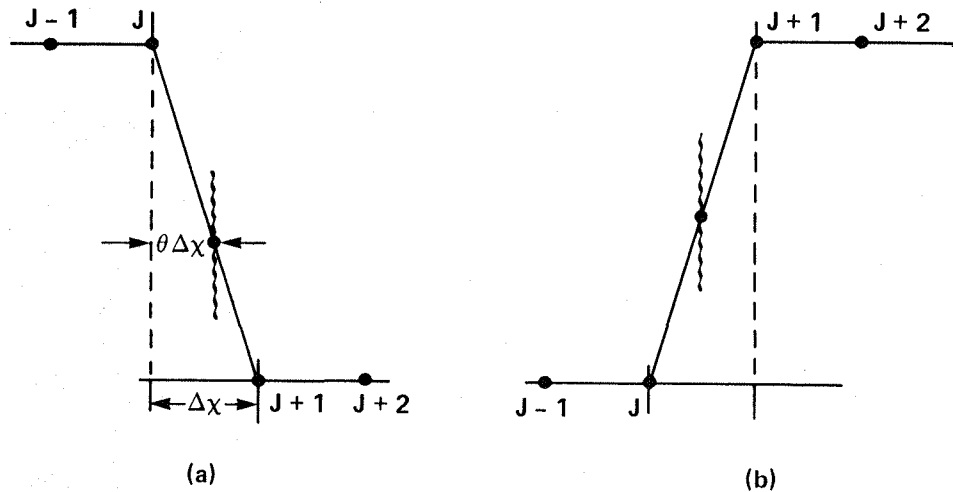
Figure 1.- Transonic shock transitions.   (a) Transonic shock; (b) transonic expansion.
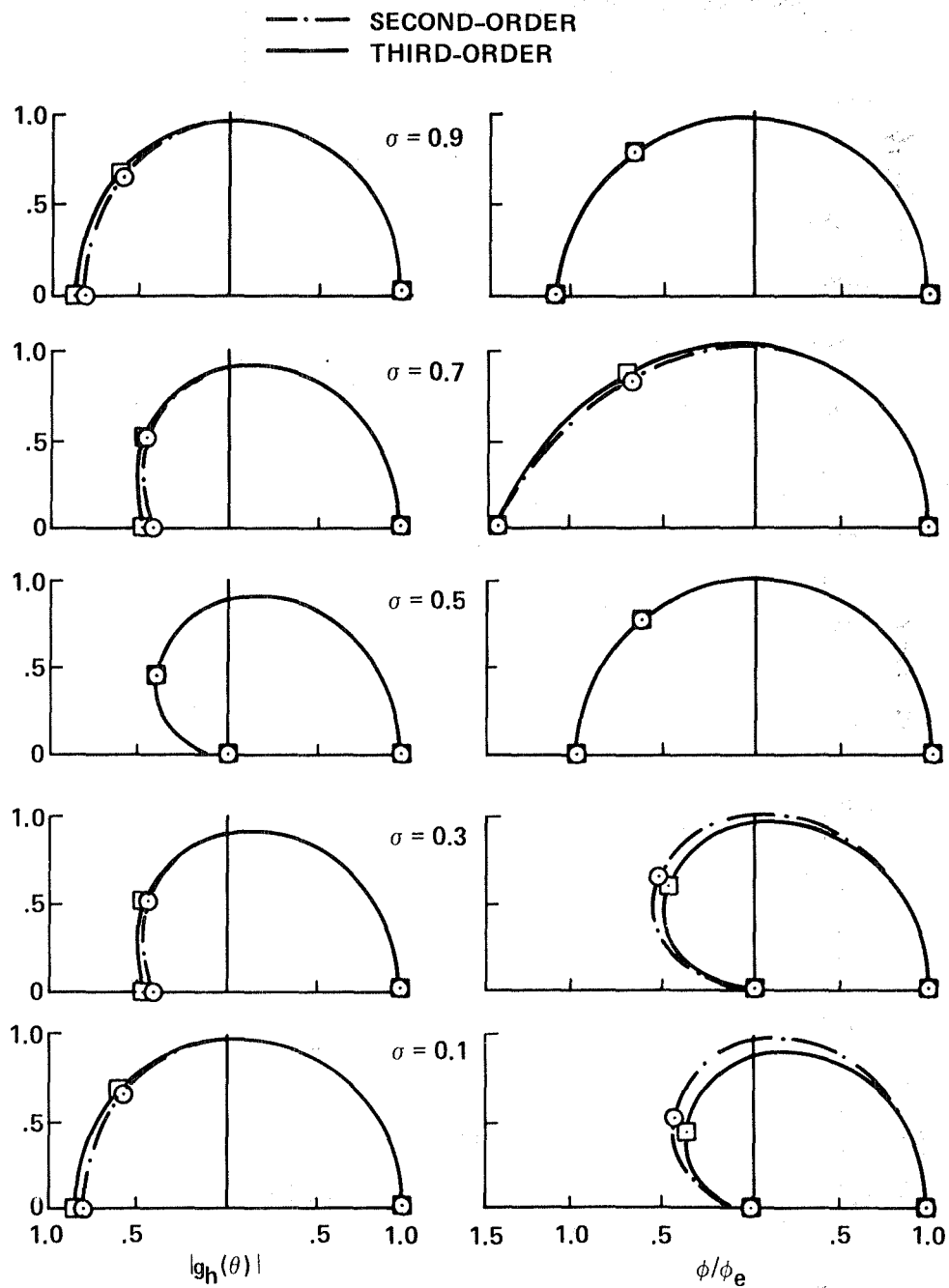
Figure 2.- Comparison of amplification factor modulus $|g_h(\theta)|$ and phase error ϕ/ϕ_e for second- and third-order schemes.
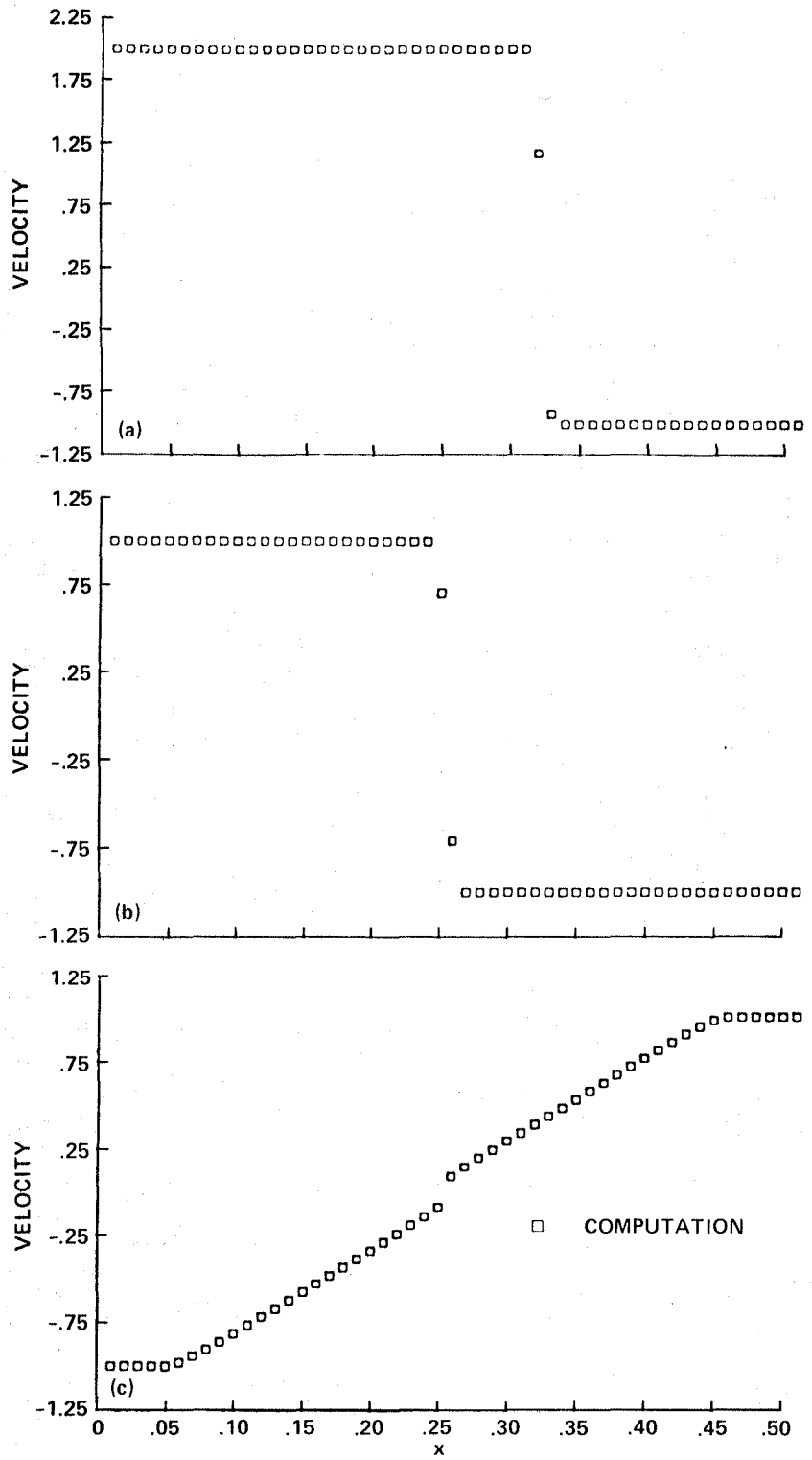
Figure 3.- Solution of the Burgers Equation (first-order). (a) Stationary shock; (b) moving shock; (c) transonic expansion.
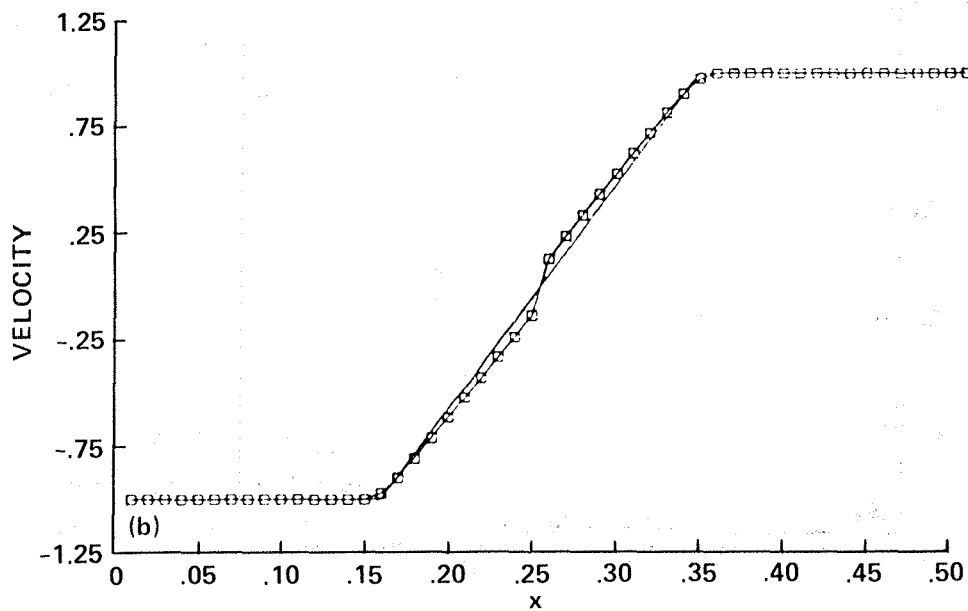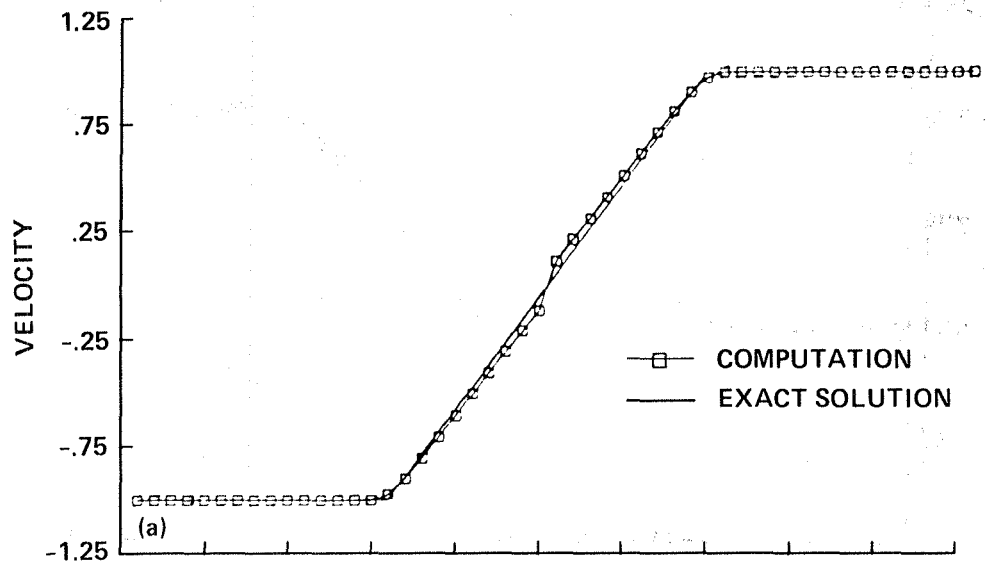
Figure 4.- Solution of the Burgers Equation. (a) Transonic expansion (second-order, IIa); (b) transonic expansion (third-order, IIIa).
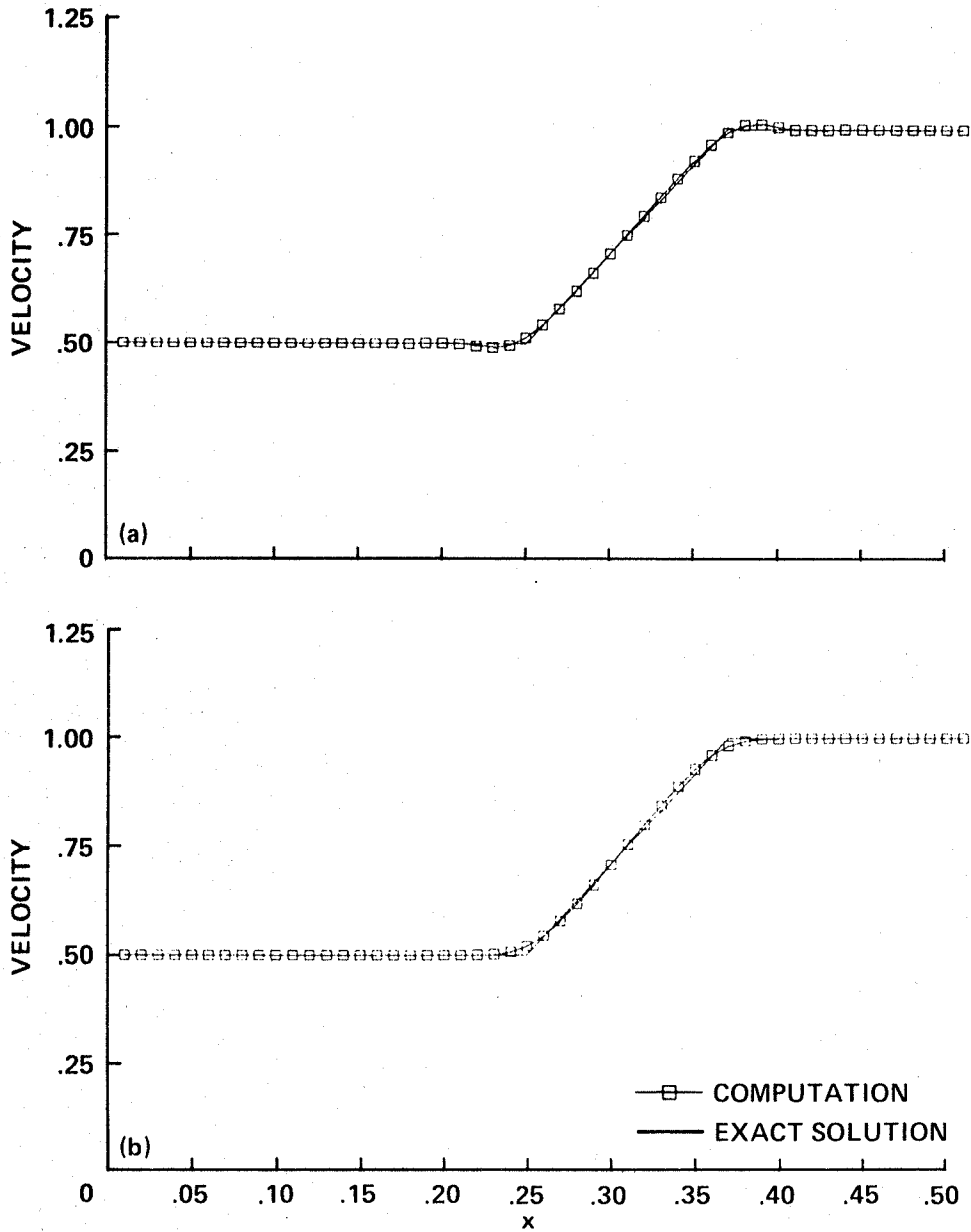
Figure 5.- Fully supersonic expansion. (a) Second-order, II; (b) second-order, IIa; (c) third-order, III; (d) third-order, IIIa.
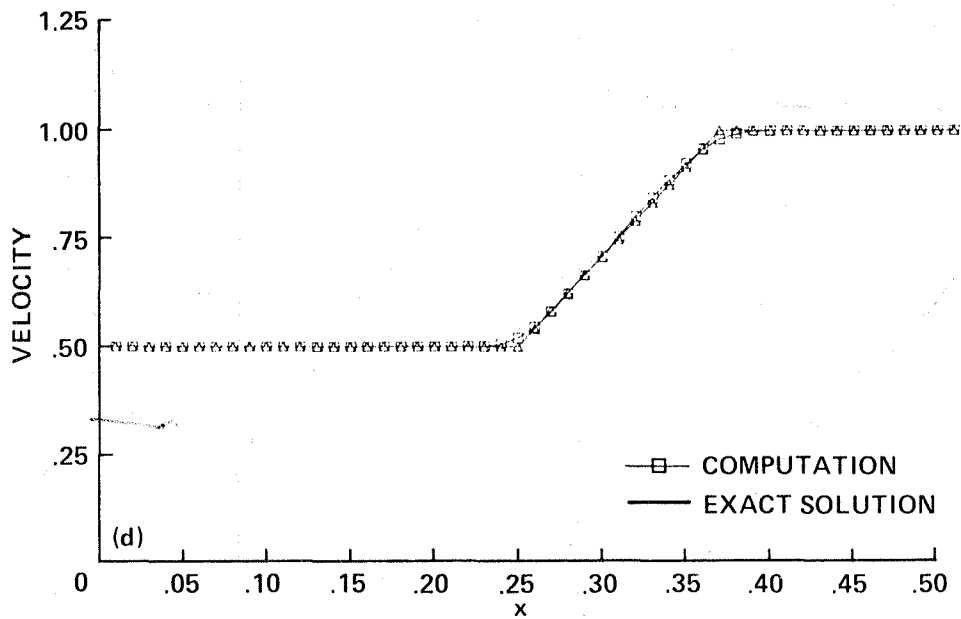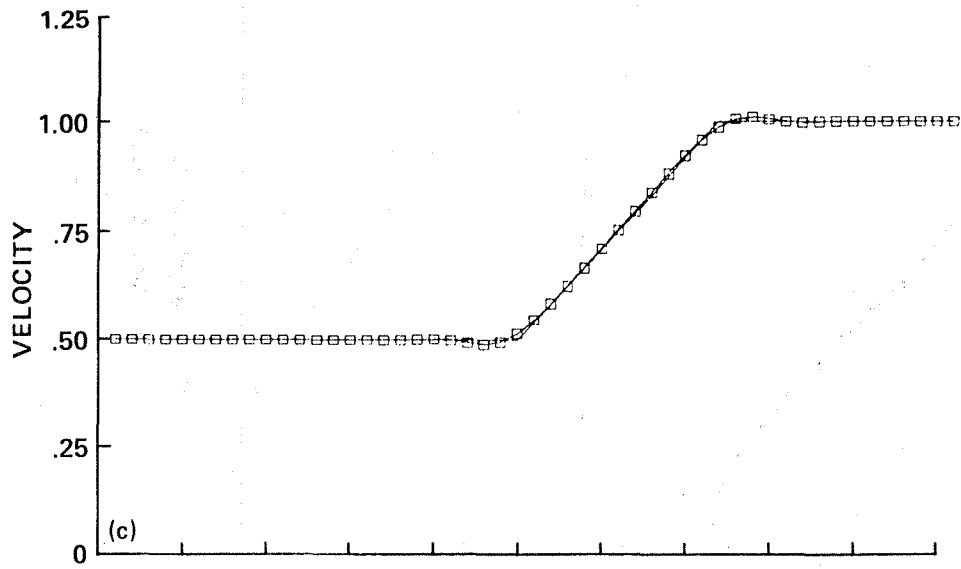
Figure 5.- Concluded.
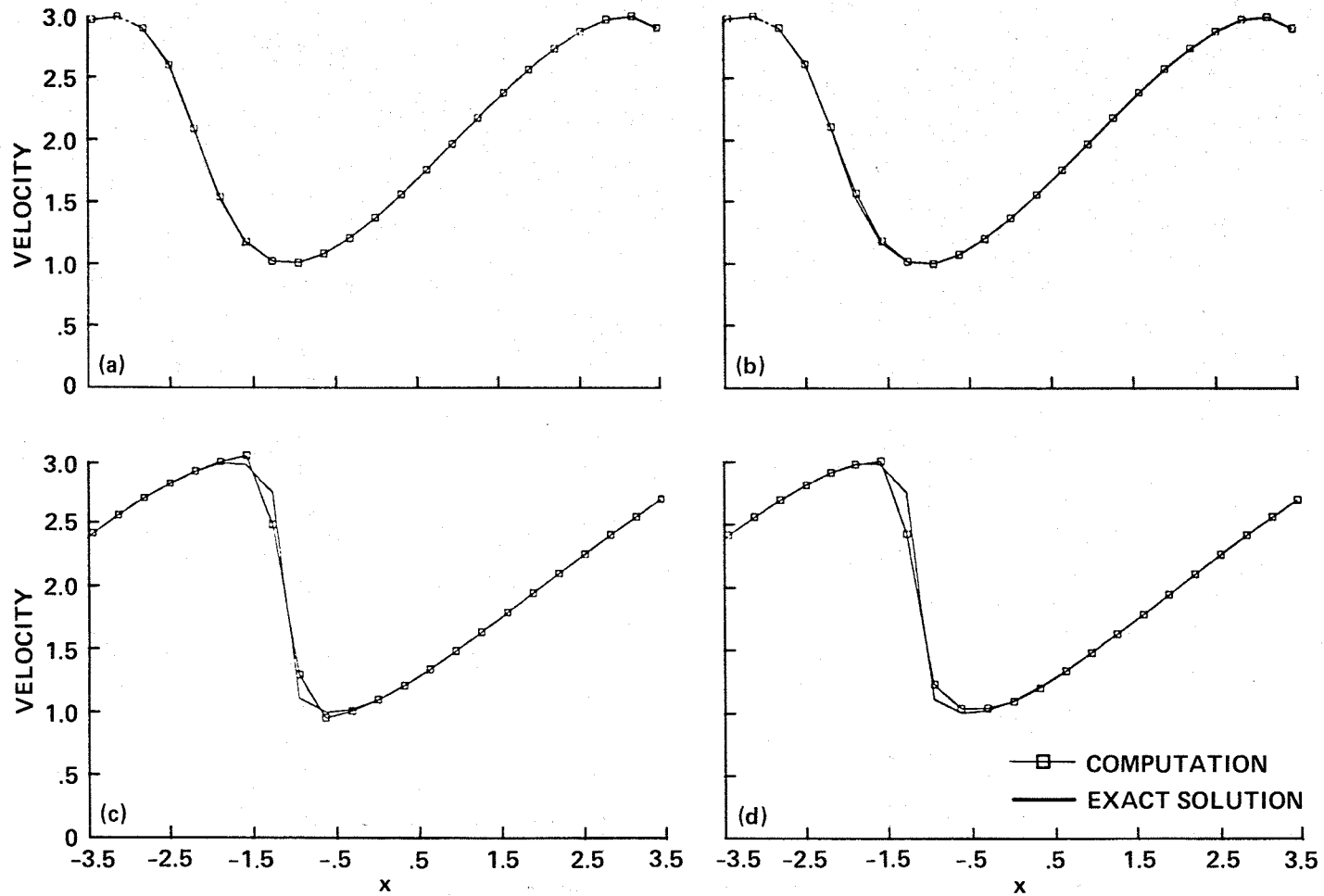
Figure 6.— Solution of the Burgers equation. (a) Smooth solution (II); (b) smooth solution (IIa);
(c) shock solution (II); (d) shock solution (IIa).
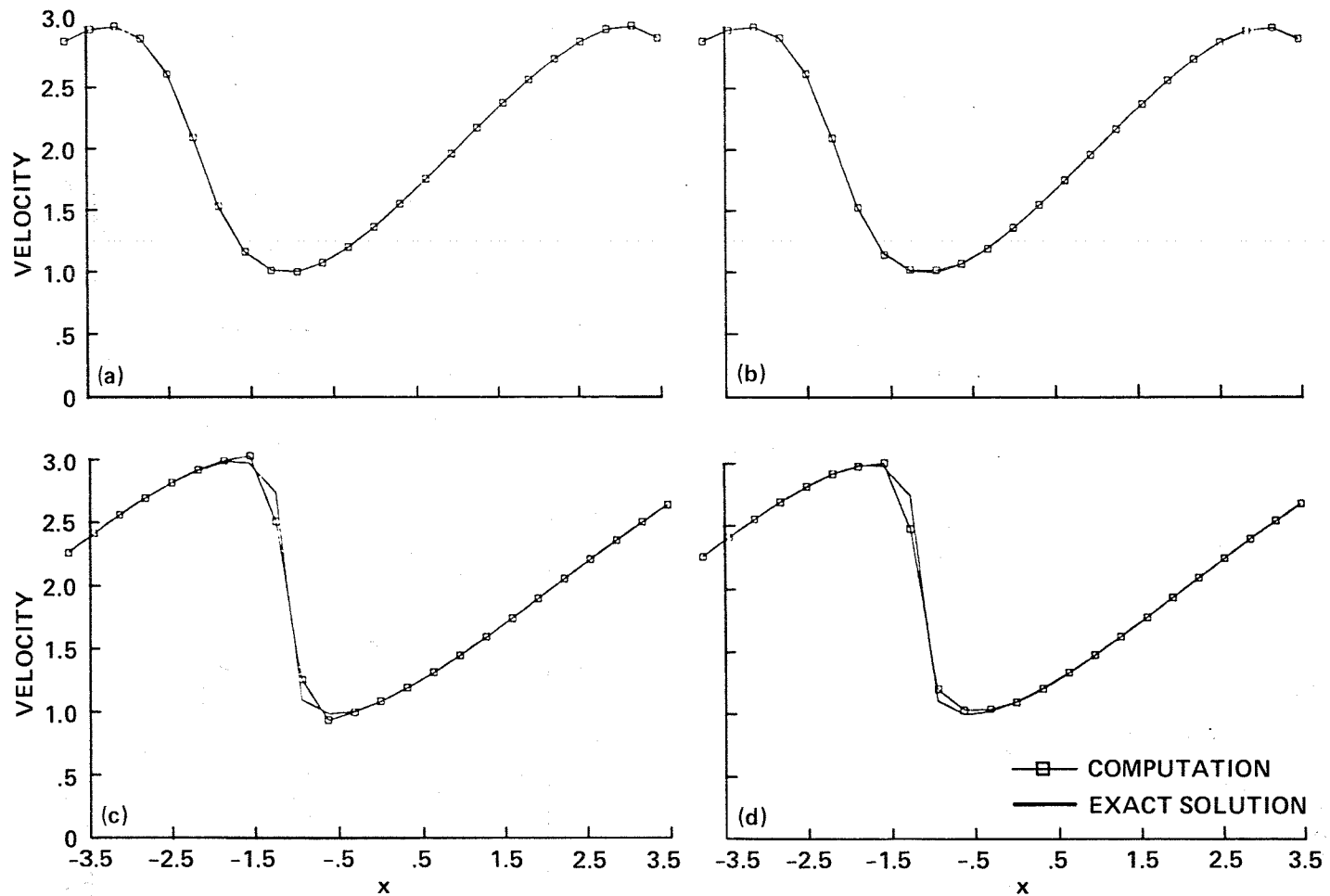
Figure 7.- Solution of the Burgers equation. (a) Smooth solution (III); (b) smooth solution (IIIa); (c) shock solution (III); (d) shock solution (IIIa).
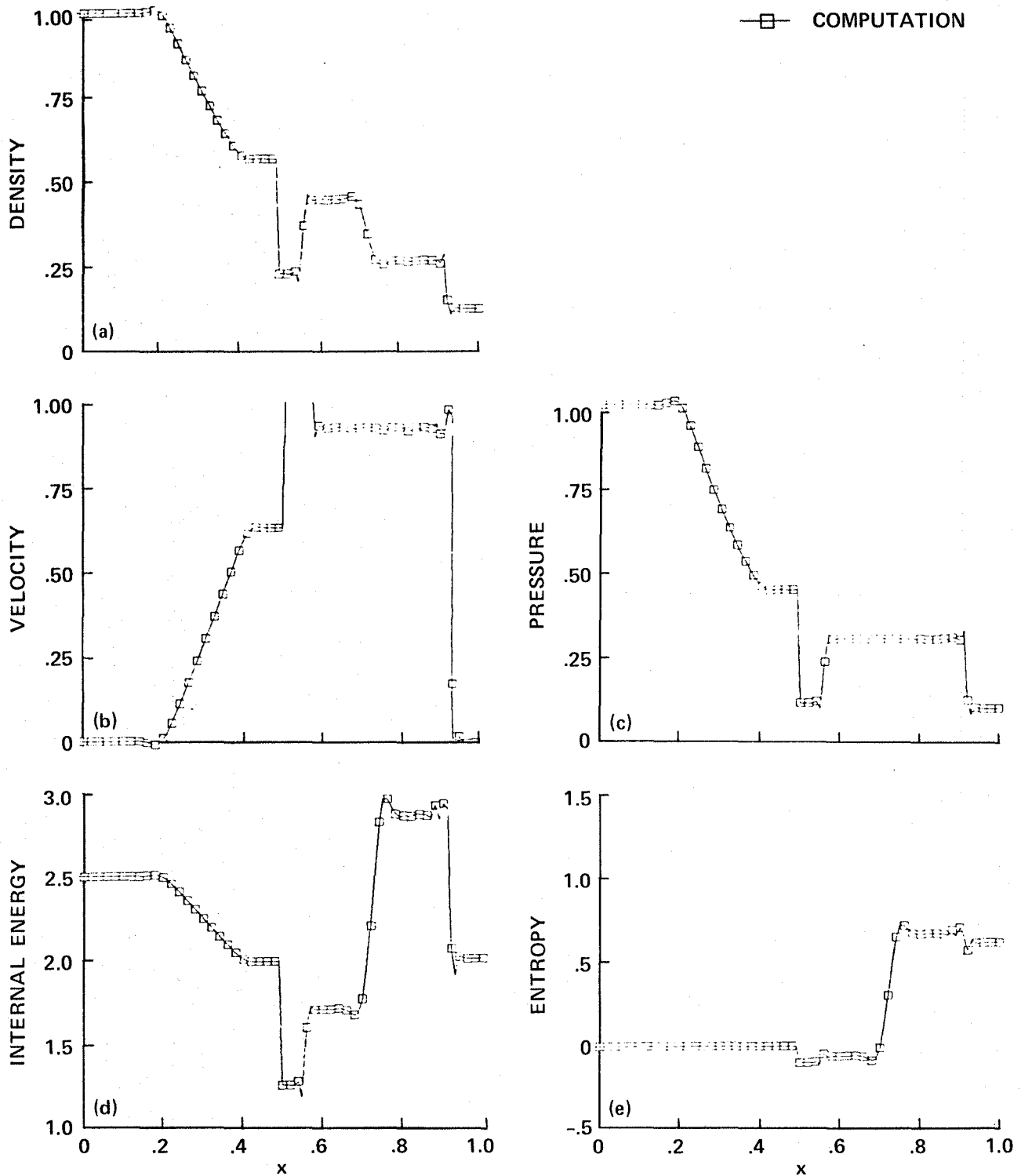
Figure 8.- Ideal shock tube solution (second-order, II). (a) Density; (b) velocity; (c) pressure; (d) internal energy; (e) entropy.
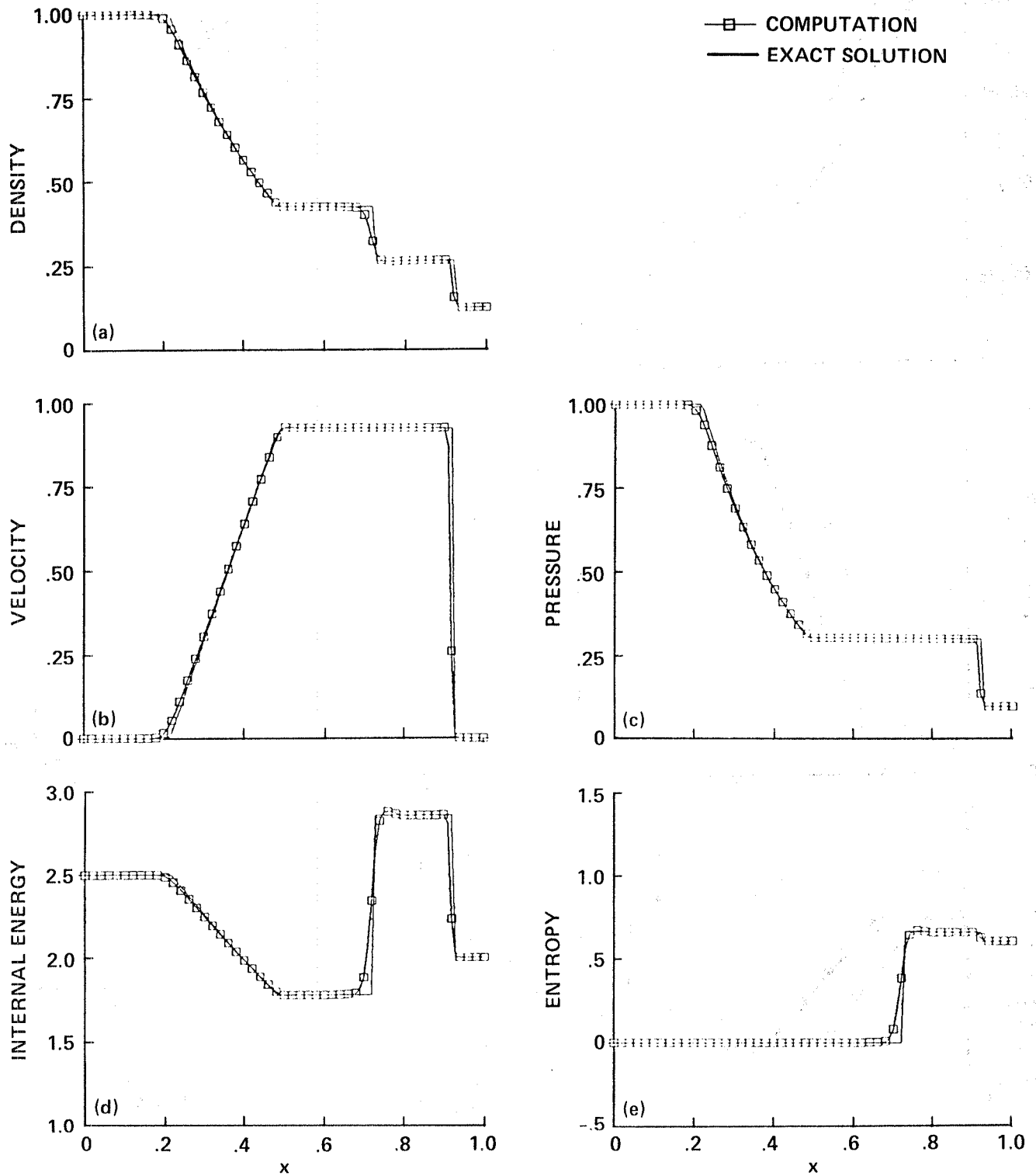
Figure 9.- Ideal shock tube solution (second-order, IIa). (a) Density; (b) velocity; (c) pressure; (d) internal energy; (e) entropy.
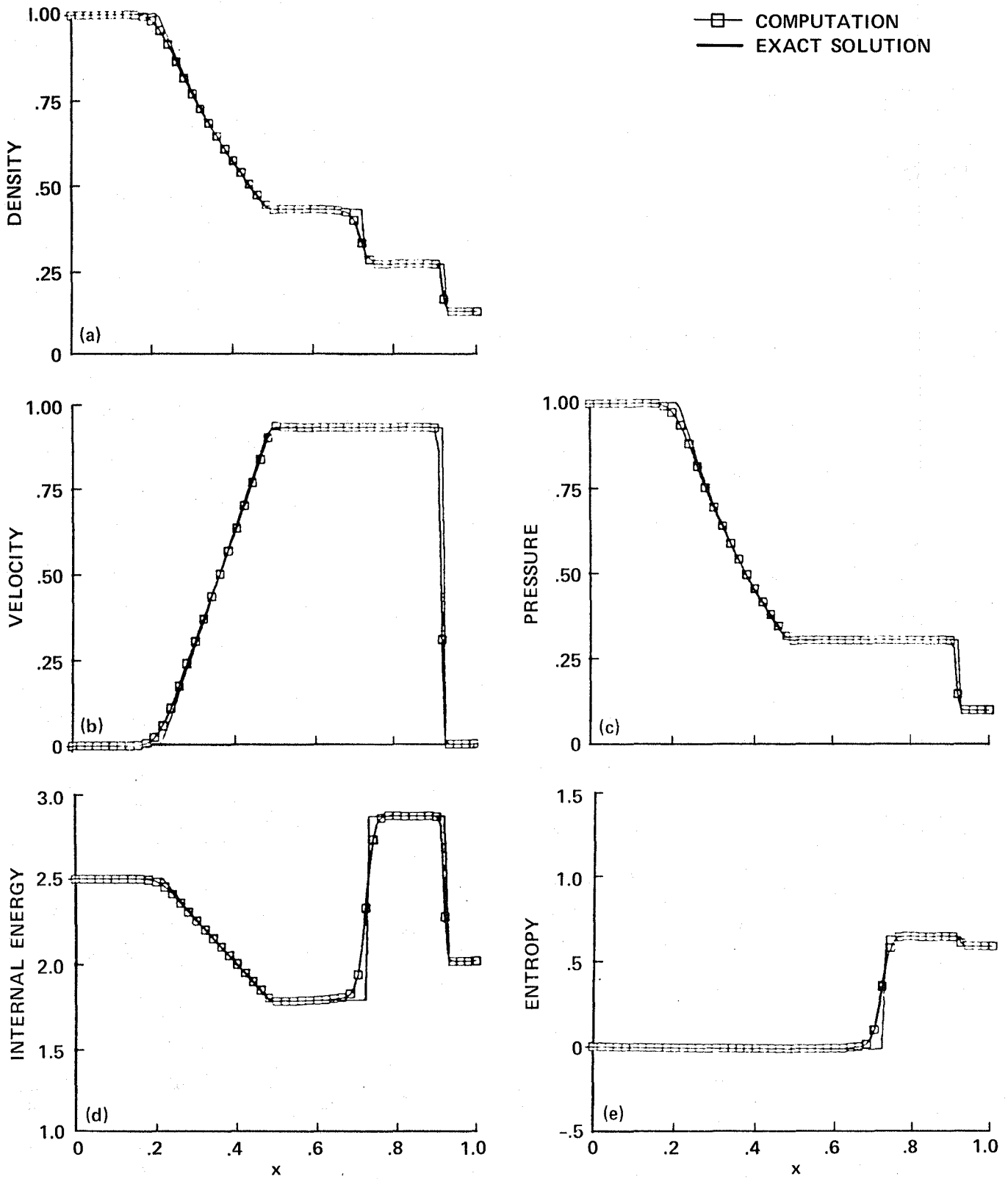
Figure 10.- Ideal shock tube solution (second-order, IIb). (a) Density;
(b) velocity; (c) pressure; (d) internal energy; (e) entropy.

36
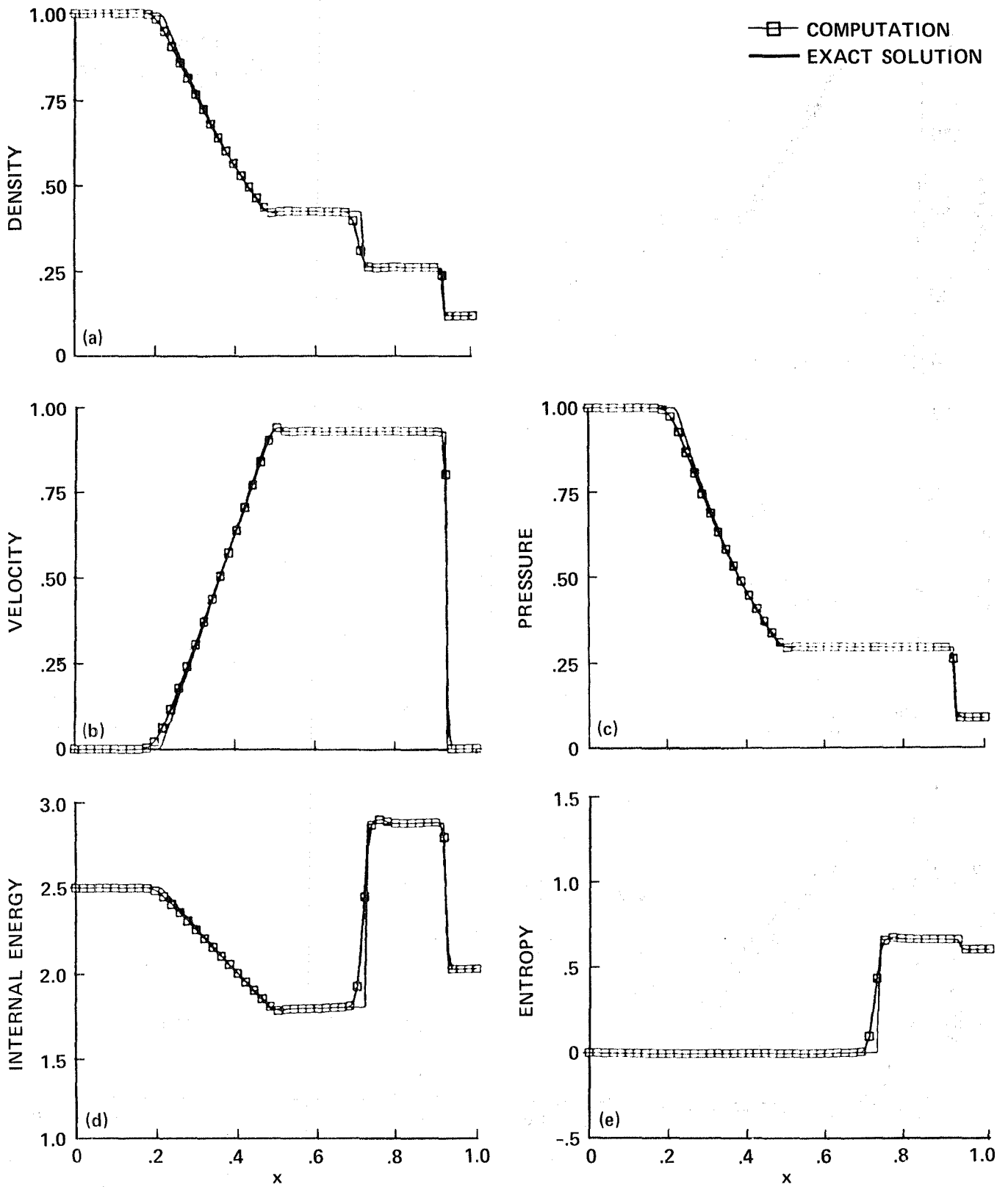
Figure 11.- Ideal shock tube solution (third-order, IIIa). (a) Density;
(b) velocity; (c) pressure; (d) internal energy; (e) entropy.
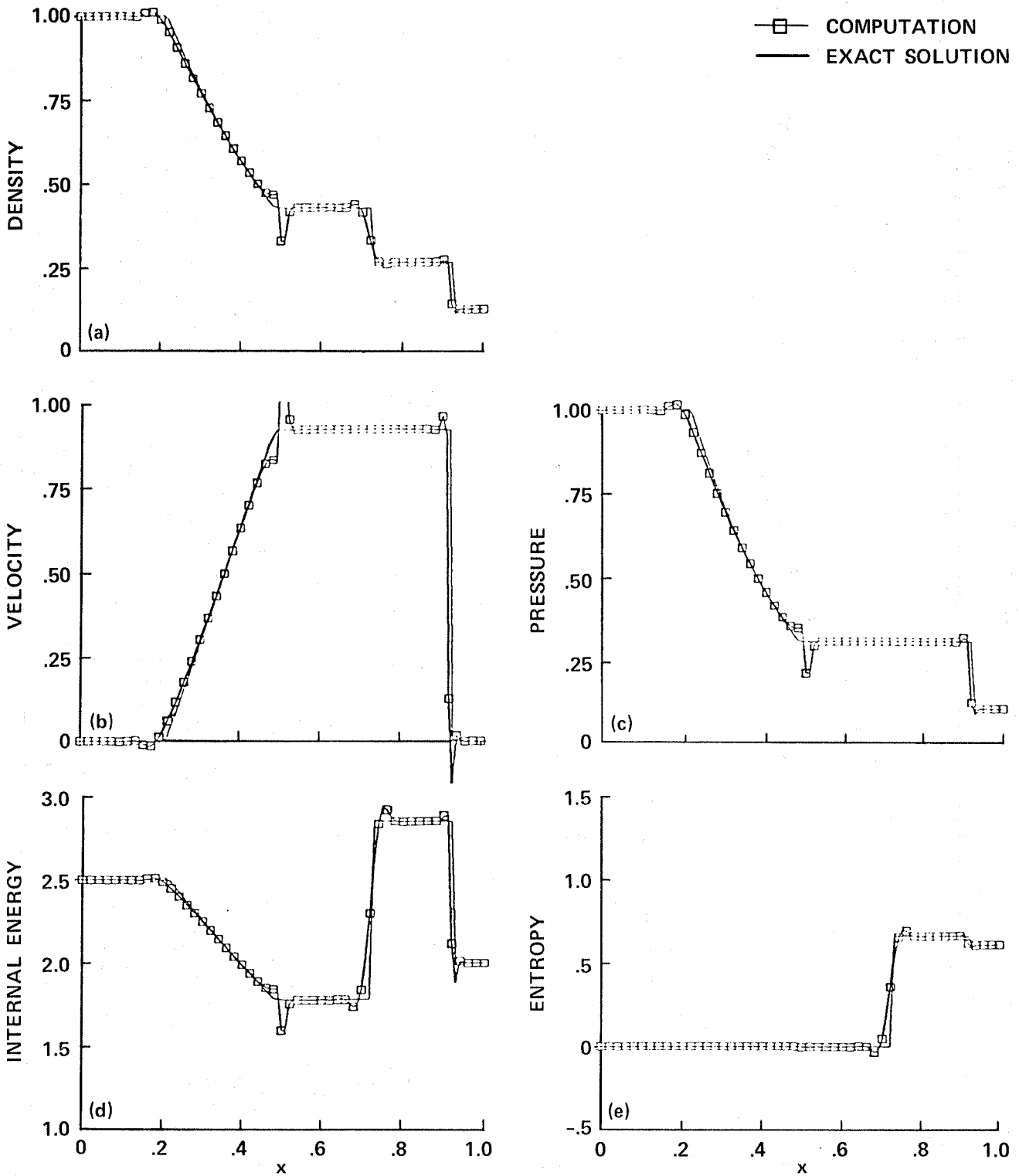
Figure 12.- Ideal shock tube solution (third-order, III). (a) Density;
(b) velocity; (c) pressure; (d) internal energy; (e) entropy.

38
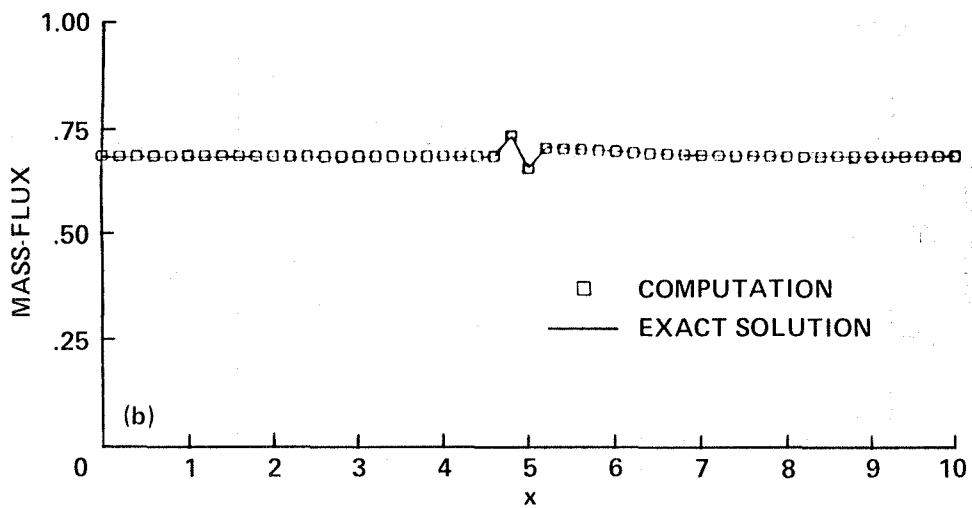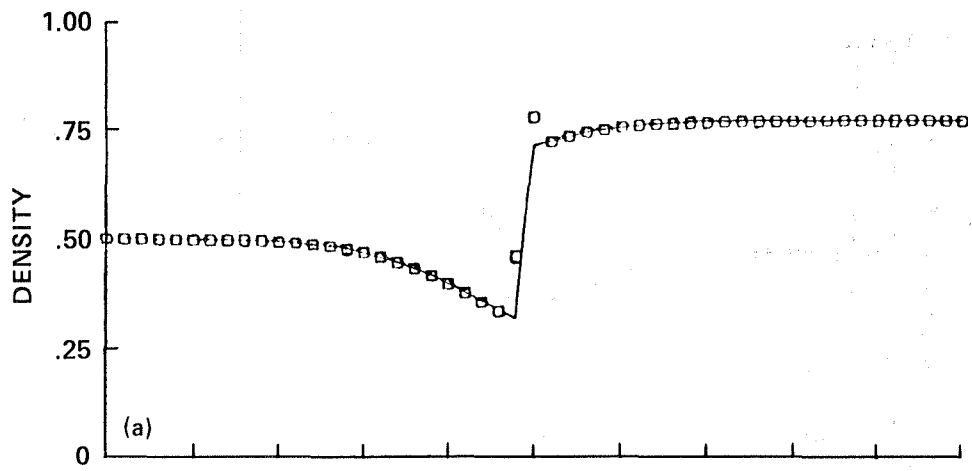
Figure 13.- Divergent nozzle (explicit first-order, without shock operator).
(a) Density; (b) mass flux.
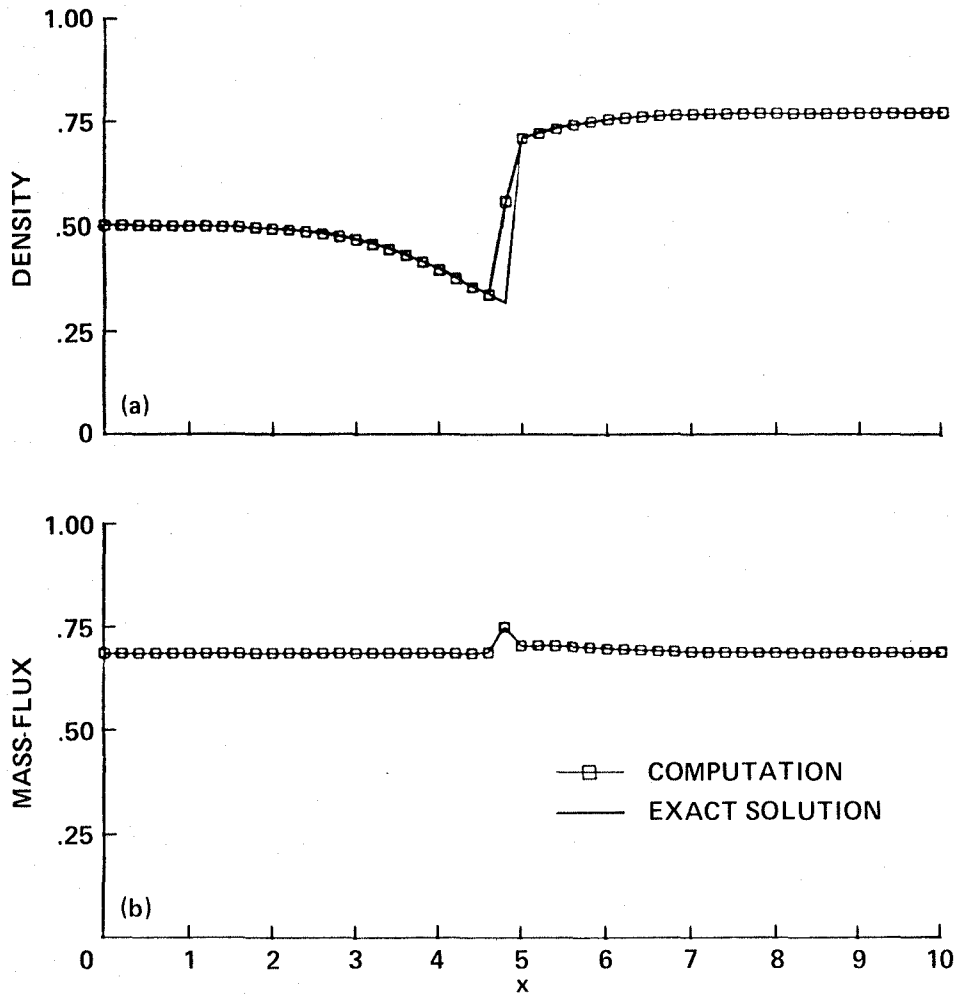
Figure 14.- Divergent nozzle (explicit first-order, with shock operator).
(a) Density; (b) mass flux.
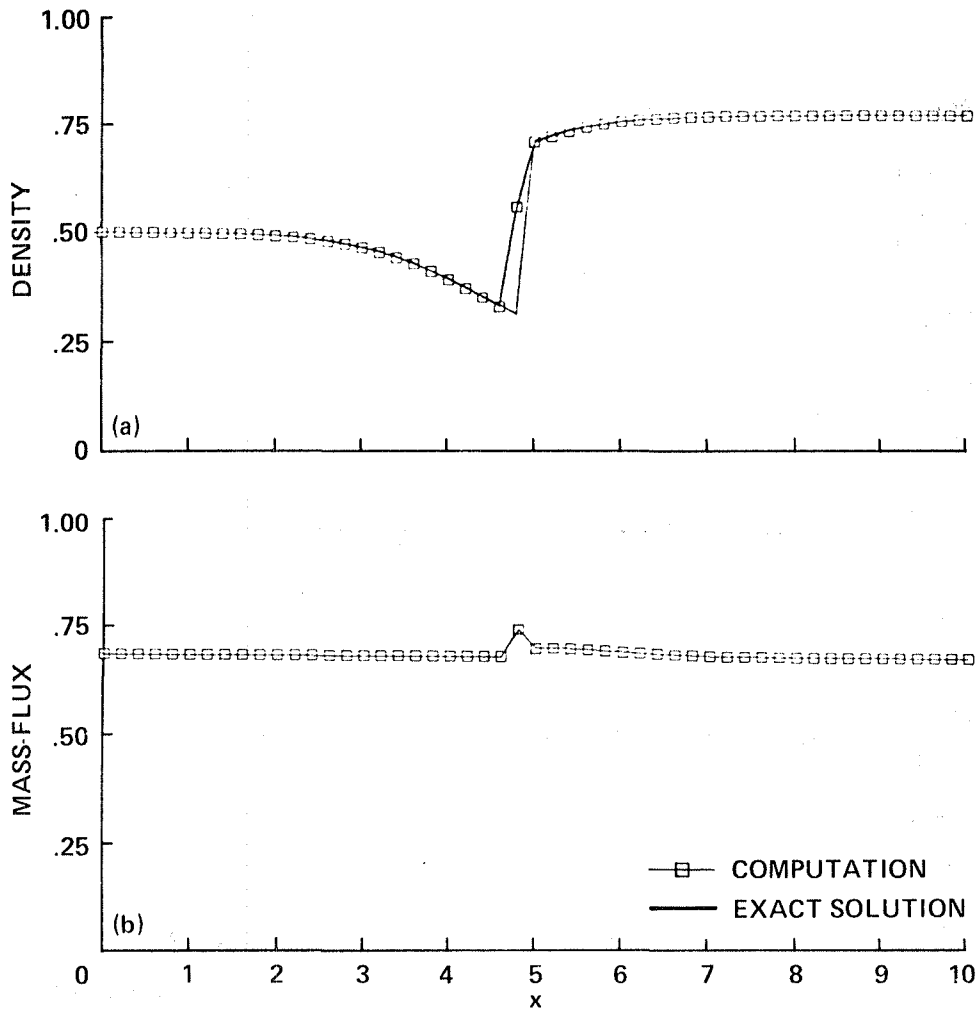
Figure 15.- Divergent nozzle (implicit first-order, with shock operator).
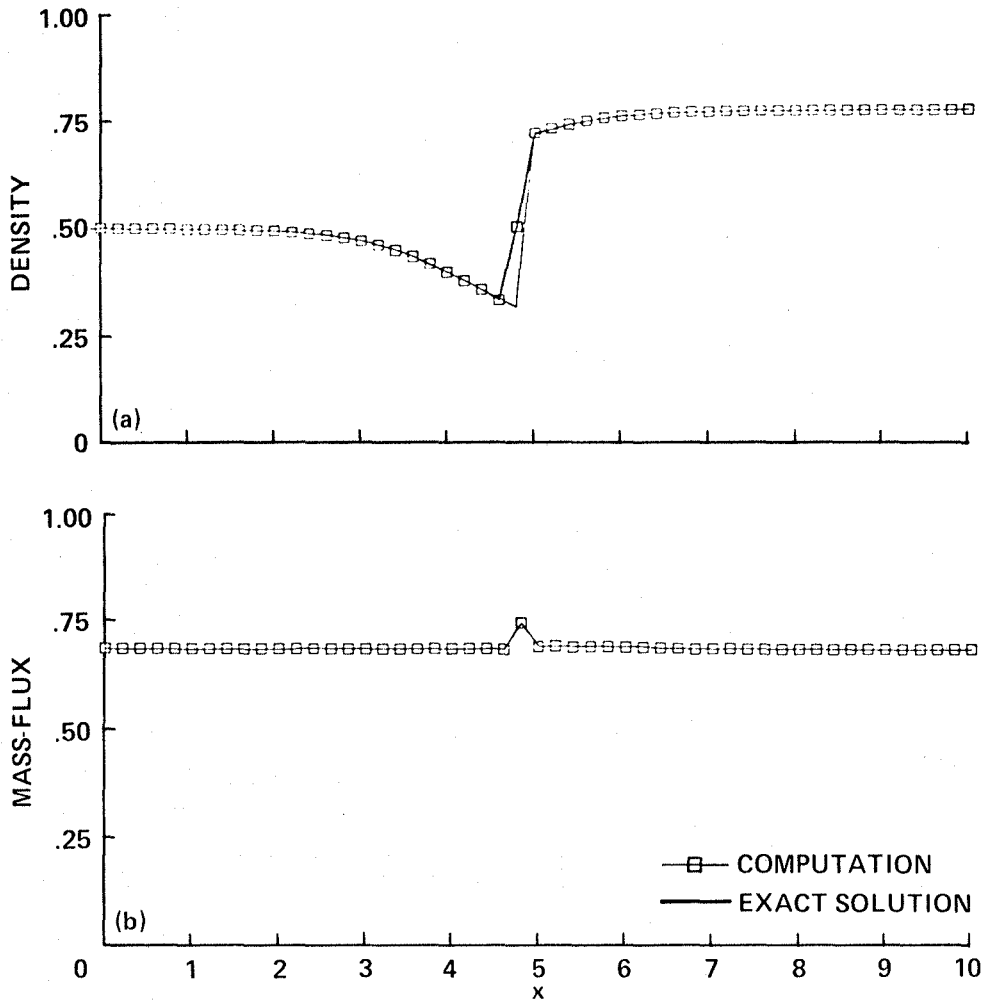(a) Density; (b) mass flux.

Figure 16.- Divergent nozzle (explicit second-order, with (6-11) and (6-12)).
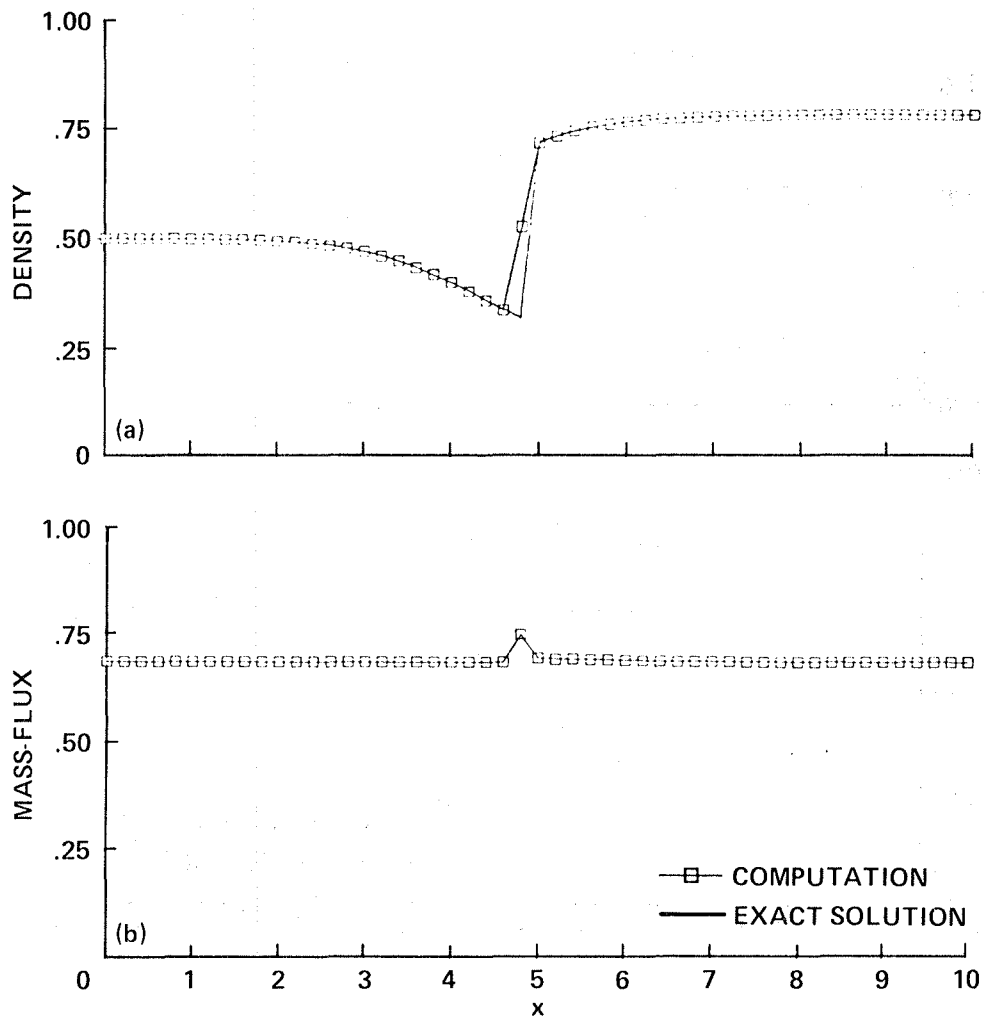(a) Density; (b) mass flux.

42

Figure 17.- Divergent nozzle (explicit second-order, with shock operator).
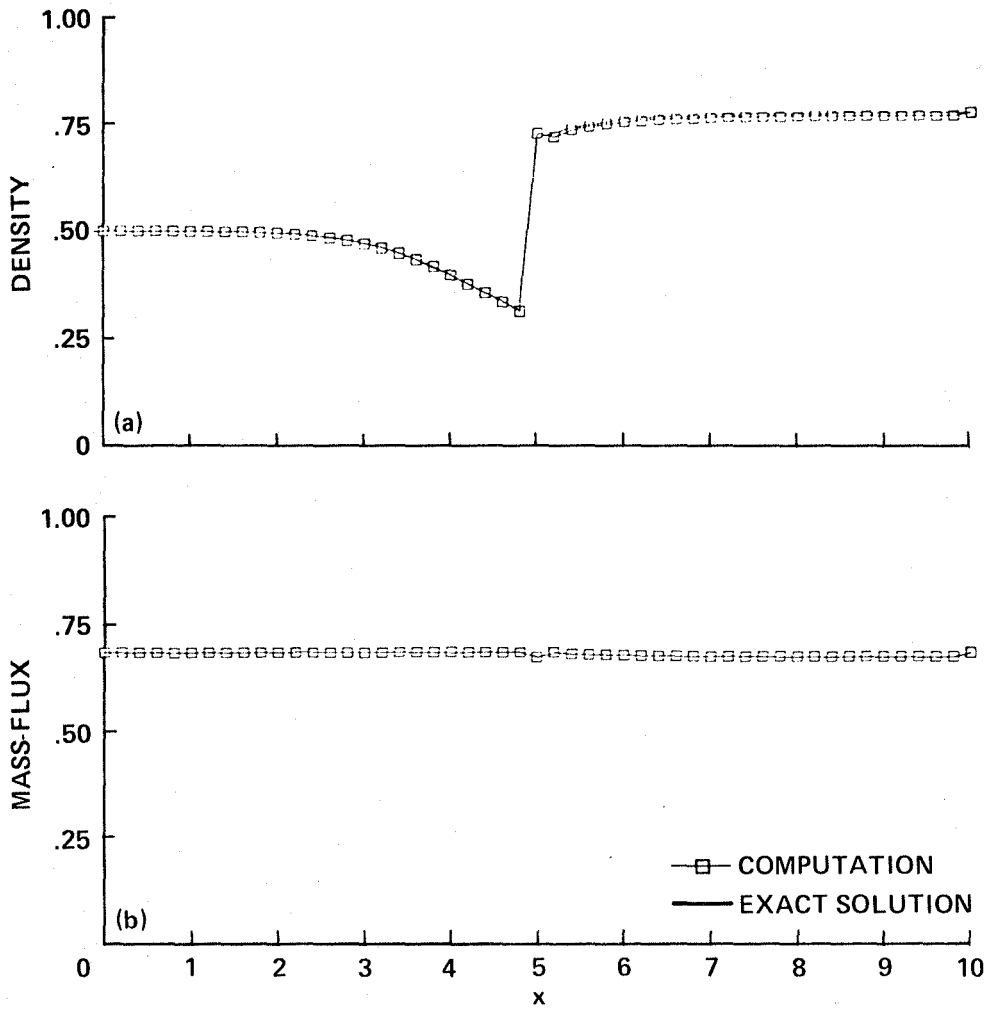(a) Density; (b) mass flux.

Figure 18.- Divergent nozzle (explicit third-order, with (6-11) and (6-12)).
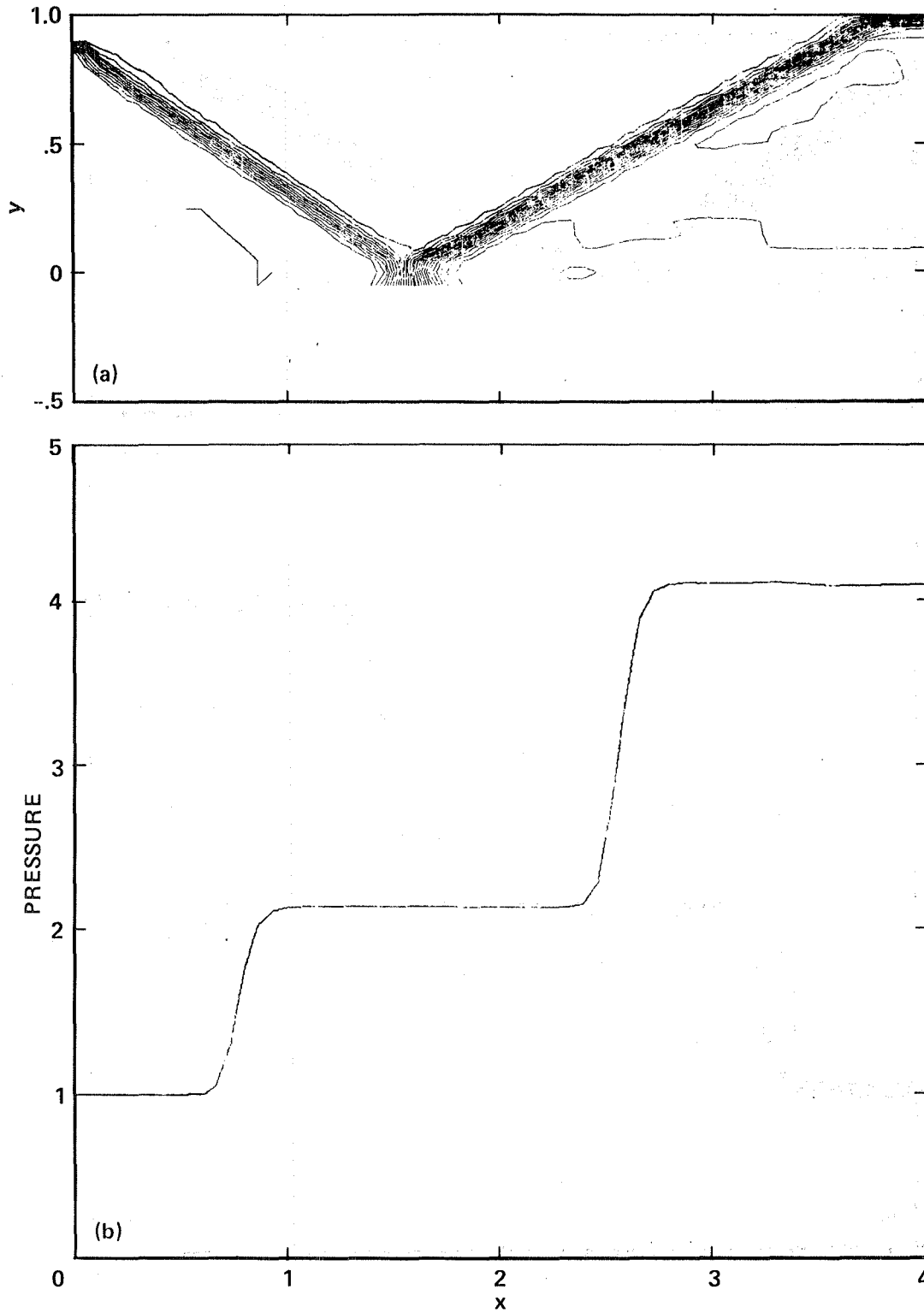(a) Density; (b) mass flux.

Figure 19.- Regular shock reflection (scheme IIa). (a) Density contours;
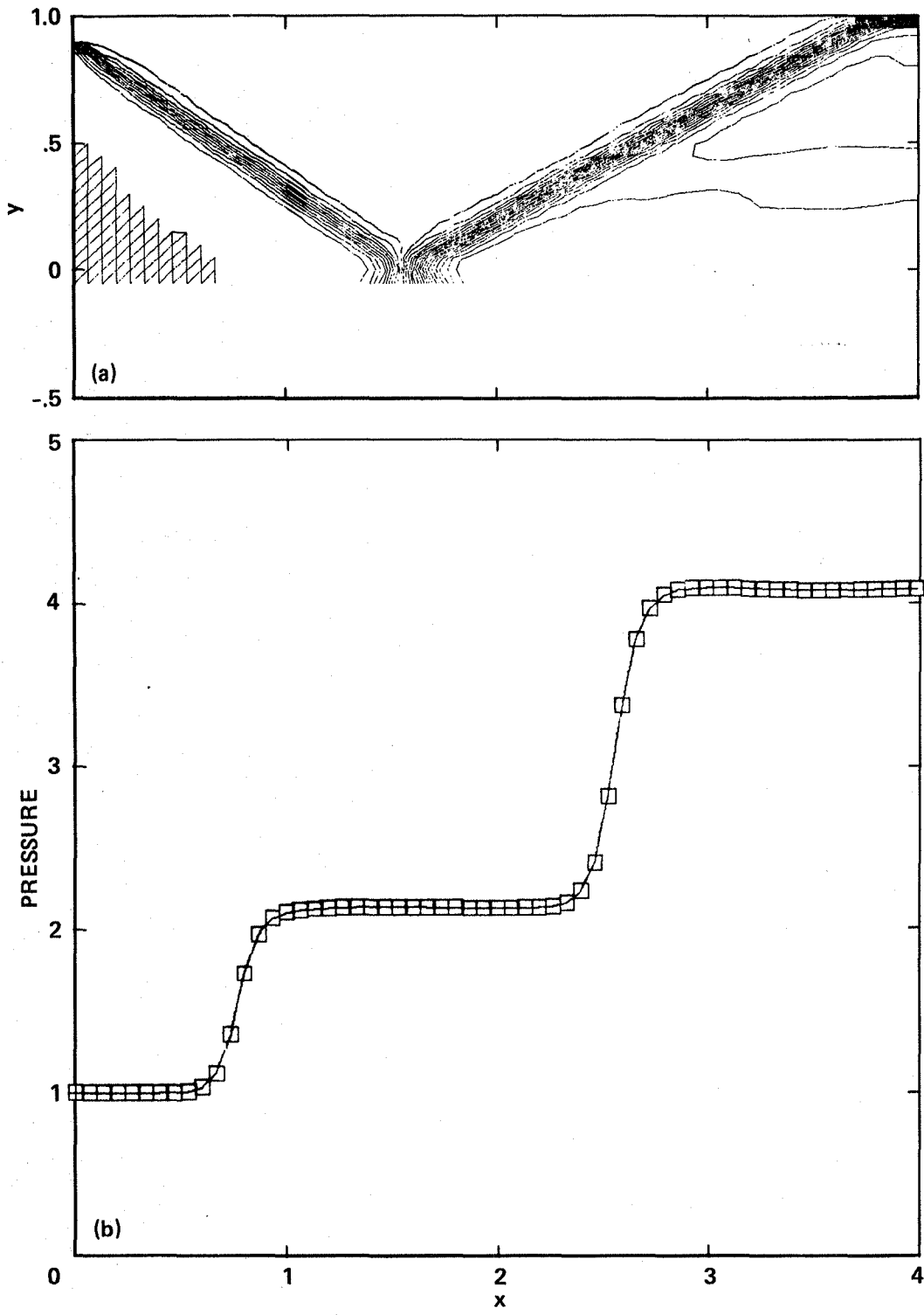(b) pressure distribution at y = 0.5.

Figure 20.- Regular shock reflection (scheme IIb). (a) Density contours; (b) pressure distribution at y = 0.5.

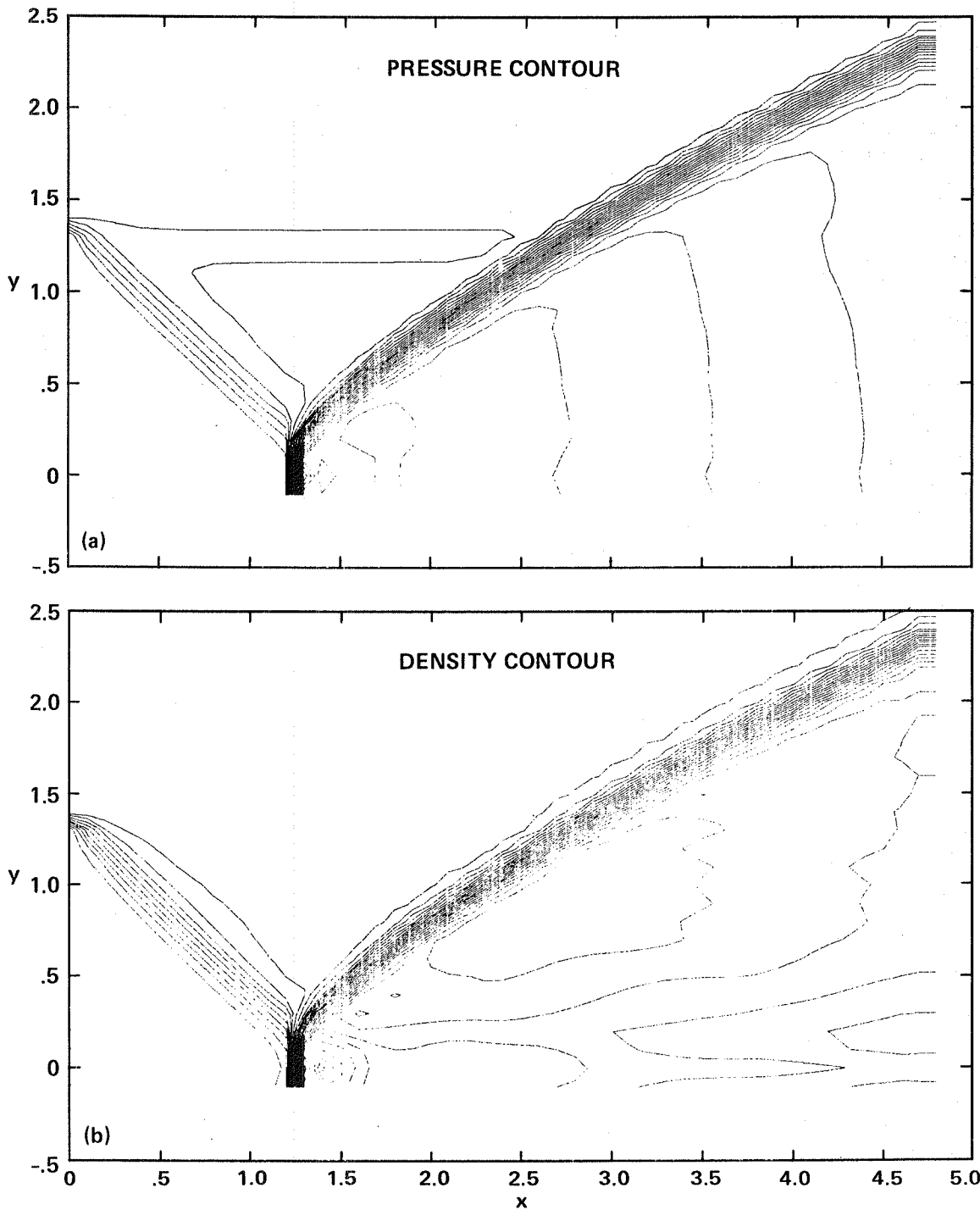Figure 21.- Simple Mach reflection (scheme IIa). (a) Pressure contours;
(b) density contours.

1. Report No. NASA TM-85959	2. Government Accession No.	3. Recipient's Catalog No.

4. Title and Subtitle	5. Report Date
SECOND- AND THIRD-ORDER UPWIND DIFFERENCE SCHEMES FOR THE EULER EQUATIONS OF GAS DYNAMICS	July 1984
	6. Performing Organization Code ATP

7. Author(s)	8. Performing Organization Report No.
Jaw-Yen Yang	A-9752
	10. Work Unit No. T-6465

9. Performing Organization Name and Address	11. Contract or Grant No.
NASA Ames Research Center Moffett Field, CA 94035	
	13. Type of Report and Period Covered Technical Memorandum

12. Sponsoring Agency Name and Address	14. Sponsoring Agency Code
National Aeronautics and Space Administration Washington, DC 20546	505-31-01

15. Supplementary Notes

Point of Contact: J. Y. Yang, Ames Research Center, MS 202A-1, Moffett Field, CA 94035. (415) 965-6667 or FTS 448-6667.

16. Abstract

Second- and third-order two time-level five-point explicit upwind-difference schemes are described for the numerical solution of hyperbolic systems of conservation laws and applied to the Euler equations of inviscid gas dynamics. Nonlinear smoothing techniques are used to make the schemes total variation diminishing. In the method both hyperbolicity and conservation properties of the hyperbolic conservation laws are combined in a very natural way by introducing a normalized Jacobian matrix of the hyperbolic system. Entropy satisfying shock transition operators which are consistent with the upwind differencing are locally introduced when transonic shock transition is detected. Schemes thus constructed are suitable for shock-capturing calculations. The stability and the global order of accuracy of the proposed schemes are examined. Numerical experiments for the inviscid Burgers equation and the compressible Euler equations in one and two space dimensions involving various situations of aerodynamic interest are included and compared. Numerical results using second-order schemes indicate that the stationary shock can be captured within at most two transition zones and the contact surface can be accurately resolved and are comparable with those obtained by van Leer's and Harten's high resolution schemes. Preliminary results for one-dimensional problems using the third-order scheme are presented.

17. Key Words (Suggested by Author(s))	18. Distribution Statement
Numerical method Finite difference method Hyperbolic system of conservation laws Computational fluid dynamics	Unlimited Subject Category – 64

19. Security Classif. (of this report)	20. Security Classif. (of this page)	21. No. of Pages	22. Price*
Unclassified	Unclassified	49	A03

End of Document